

AREA
NU
Church
McCoy
Case Study
P. 2

GLO24221

THE MCCOY, NEVADA GEOTHERMAL PROSPECT

An Interim Case History

PART II (Figures)

by Arthur L. Lange

*Paper delivered at the Fiftieth Annual Meeting
of the Society of Exploration Geophysicists,
Houston, Texas, 17 November 1980.*

AMAX Exploration Inc.
Geothermal Branch
7100 W. 44th Avenue
Wheat Ridge, Colorado 80033

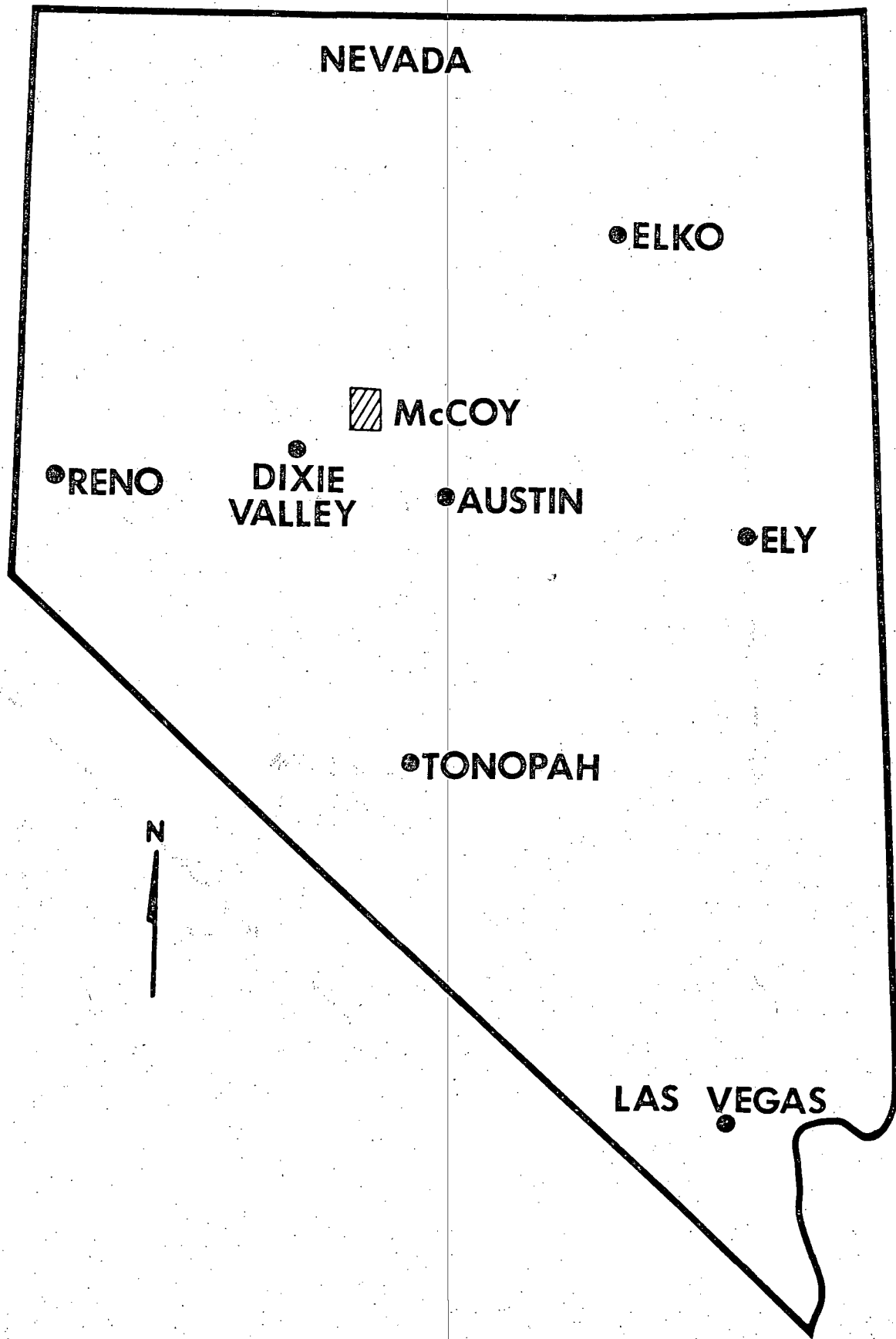
FIGURES

- 1L. Location of the McCoy prospect.
- 2R. Orientation map, showing principal features of the McCoy prospect.
- 3L. View northward from McCoy Peak.
- 4L. The McCoy mercury mine.
- 5R. Partial Landsat image showing the ring in center surrounding the McCoy prospect. Hole in the Wall wash drains the ring and empties into Dixie Valley on the west.
- 6L. Simplified geologic map, showing locations of McCoy and Wildhorse mines. PP, Permo-Pennsylvanian sediments; TRJ, Triassic-Jurassic conglomerates, carbonates and sandstones; T, Tertiary volcanics; Qal, Quaternary alluvium; Qt, Quaternary hot spring travertines. (after Pilkington, 1979).
- 7R. East-west geologic profile through McCoy mine (See Slide 9L), with profile of temperature @ 100m and conductive isotherms.
- 8L. Heatflow map showing thermal anomaly shaded, highest heatflows stippled and lowest, striped.
- 9L. Map of temperature at 100m showing thermal anomaly shaded, highest temperatures stippled, and lowest, striped.
- 10R. Profile of temperatures and isotherms along Line A (N/S).
- 11R. Profile of temperatures and isotherms with geologic section along Line C (E/W) (Geology after Pilkington, 1979).
- 12L. Isothermal section at Red Hill Hot Spring, Utah, from Chapman, Kilty & Mase, 1978. Compare with Line C isotherms.
- 13L. Complete Bouguer gravity map. Highs are stippled; lows, striped.
- 14R. Gravity profile, Line B, with automatic interpretation for densities 2.1 (checked) and 2.8gm/cm^3 (striped).
- 15R. Gravity profile, Line C, with automatic interpretation for densities 2.1 (checked) and 2.8gm/cm^3 (striped).
- 16L. Residual aeromagnetic map. Highs are stippled; lows, striped.
- 17R. Map of P-wave delays from teleseisms. Largest delays are striped; advances, stippled.
- 18L. Map of Poisson's Ratios (highs, striped; lows, stippled) showing also locations of microearthquake foci and fault-plane solutions.
- 19R. Profiles of P-wave delays and advances and Poisson's ratios along Line B.

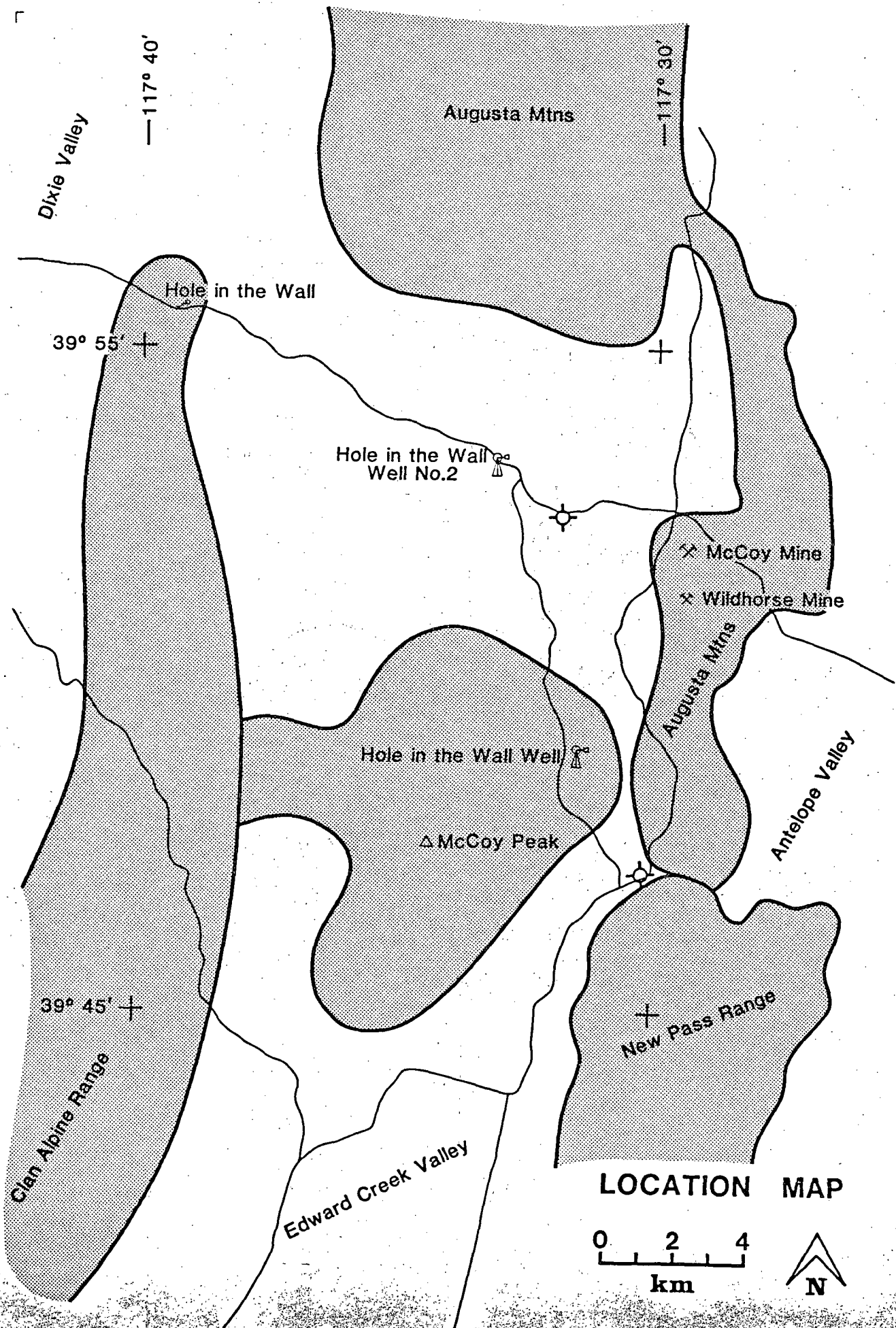
- 20R. Profiles of P-wave delays and advances and Poisson's ratios along Line C.
- 21R. Profiles of P-wave delays and advances and Poisson's ratios along Line A.
- 22L. Map of self-potential response. Negatives are striped; highs stippled.
- 23R. Refer to Figure 9L.
- 24R. Self-potential profile, Line B, compared with profile of temperature at 100m and isotherms. Microearthquake epicenters shown as stars.
- 25R. Self-potential profile, Line A, compared with profile of temperature at 100m and isotherms. Microearthquake epicenters shown as stars.
- 26R. Self-potential profile, Line C, compared with profile of temperature at 100m and isotherms. Microearthquake epicenters shown as stars.
- 27L. Resistivity at 5km depth from 1D magnetotelluric inversion (T_e mode). Conductive zones stippled; resistive striped.
- 28R. Magnetotelluric section (T_e mode, 1D inversion) along Line B compared with available EM section and geology.
- 29R. MT section (T_e mode, 1D inversion) along Line A compared with available EM data.
- 30R. MT pseudosections (resistivity vs. period) along Line C.
- 31R. MT section (T_e mode, 1D inversion) along Line C, compared with geologic section.
- 32L. Refer to Figure 8L.
- 33R. Geologic section along Line C, showing deduced geothermal reservoir feeding conduit of ascending hot water along limb of horst block. Upon encountering the Triassic conglomerate, hot water (probably cooled by cold meteoric water from the surface) drains westward--downdip--to eventually return to the deep system.

PLATES

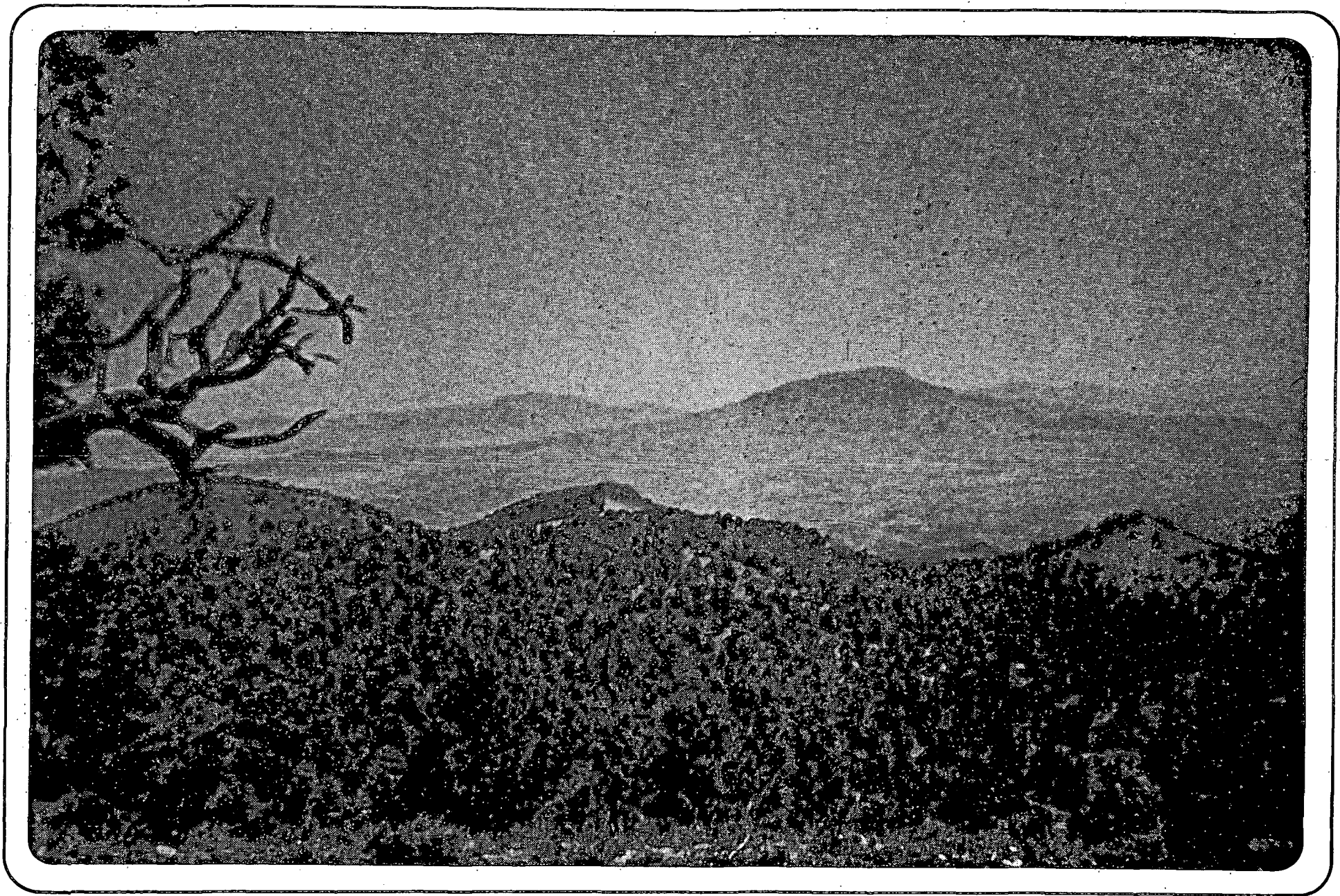
- Plate I. Stacked profiles of Line A.
- Plate II. Stacked profiles of Line B.
- Plate III. Stacked profiles of Line C.



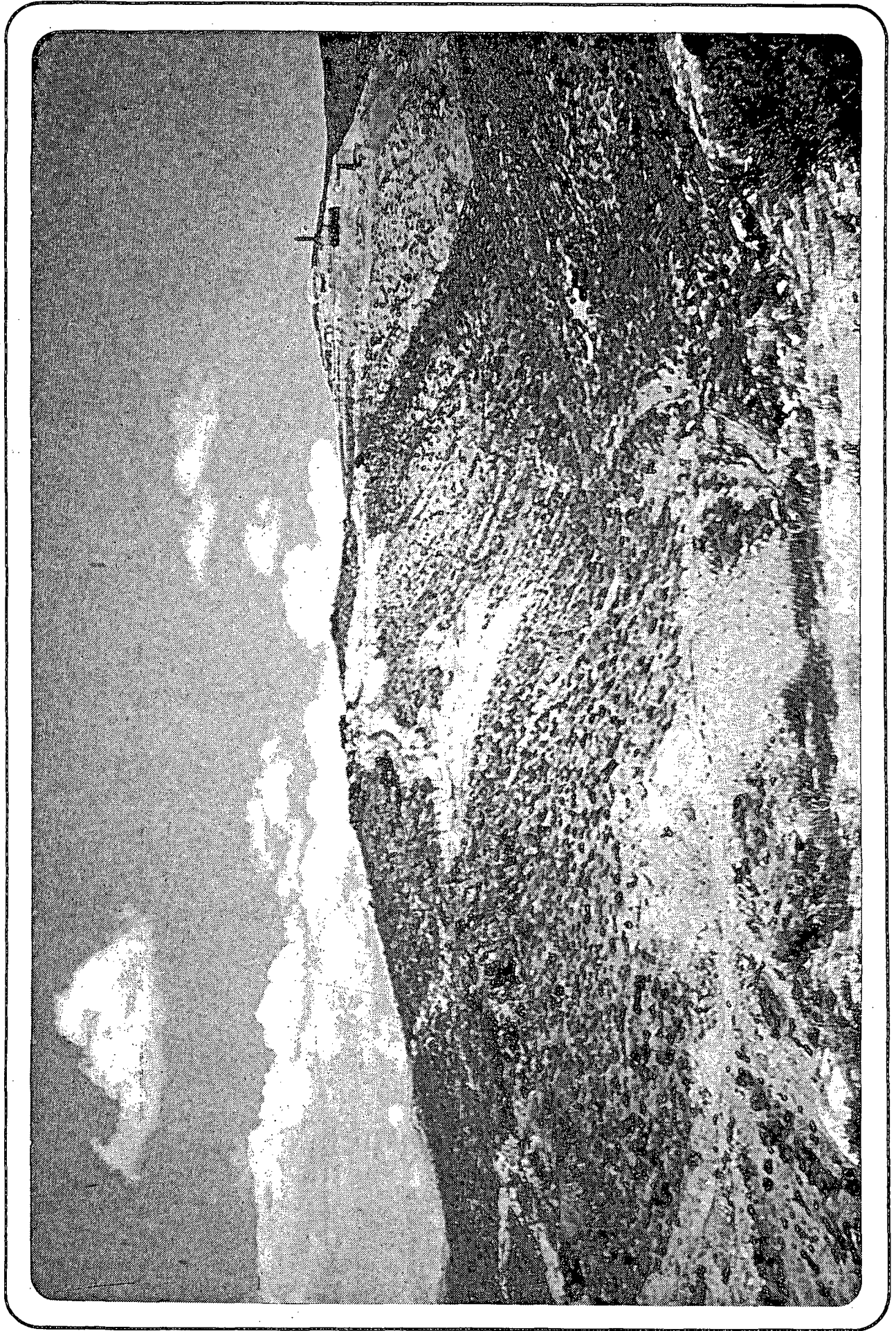
1L. Location of the McCoy prospect



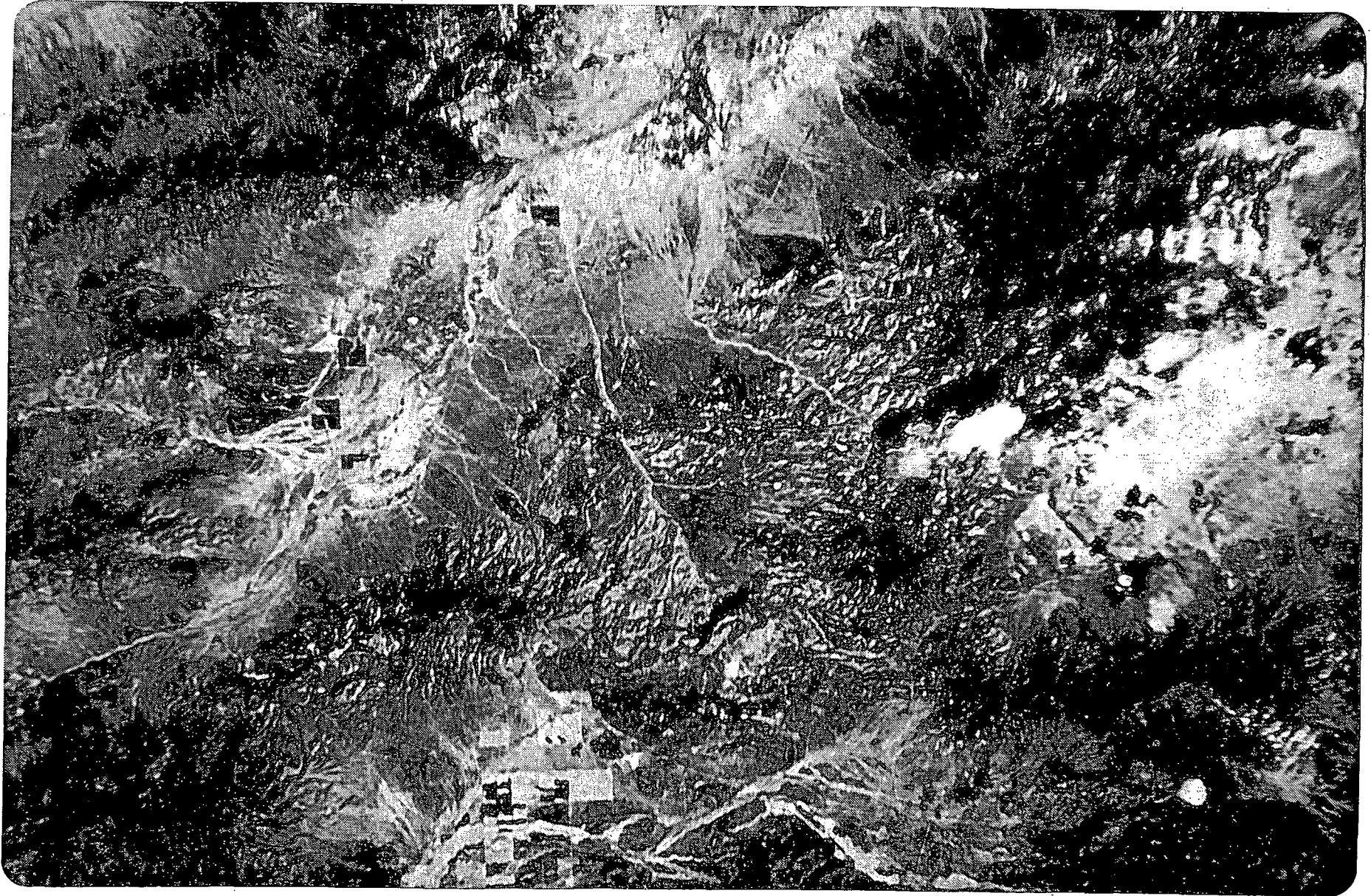
2R. Orientation map, showing principal features of the McCoy prospect



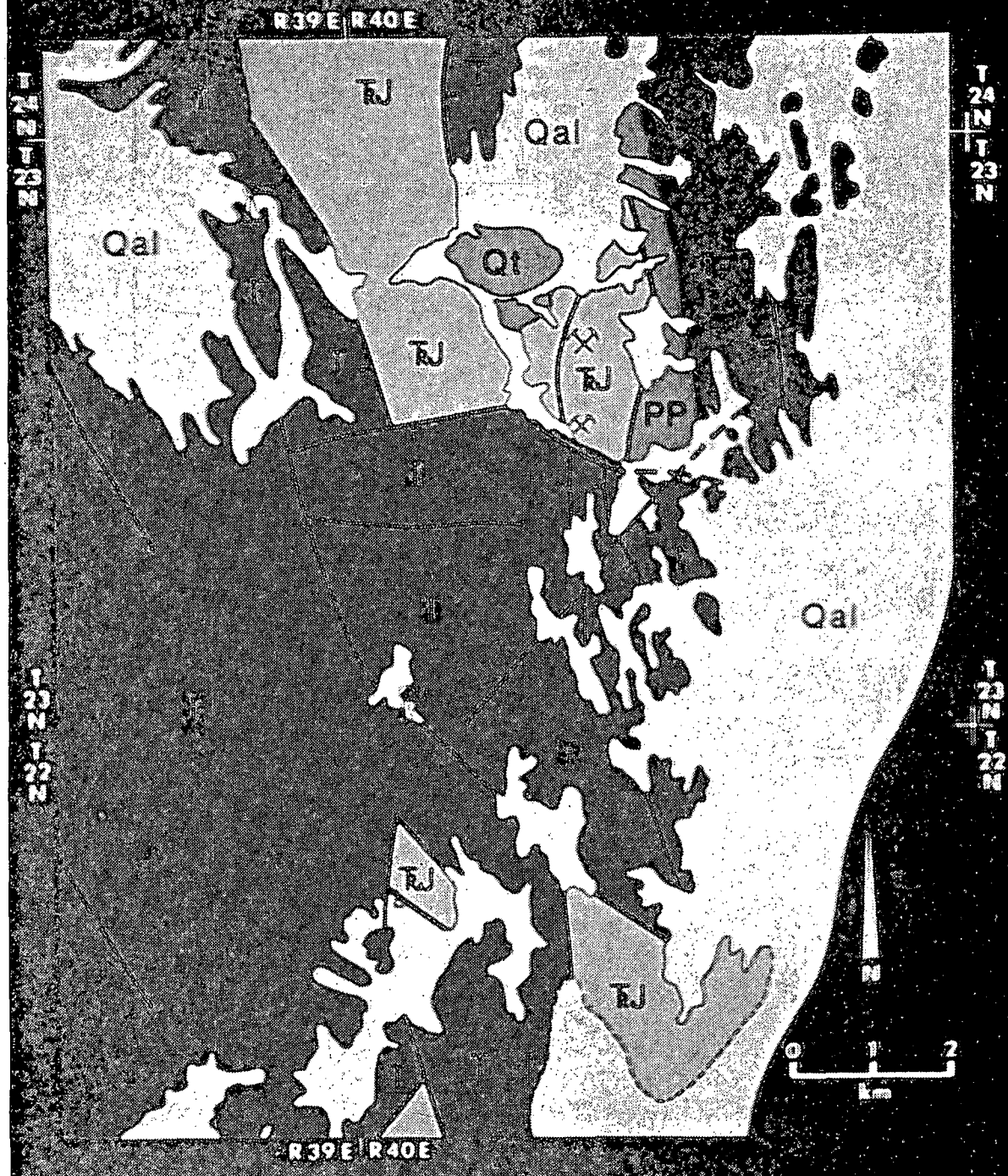
3L. View northward from McCoy Peak



4L. The McCoy mercury mine

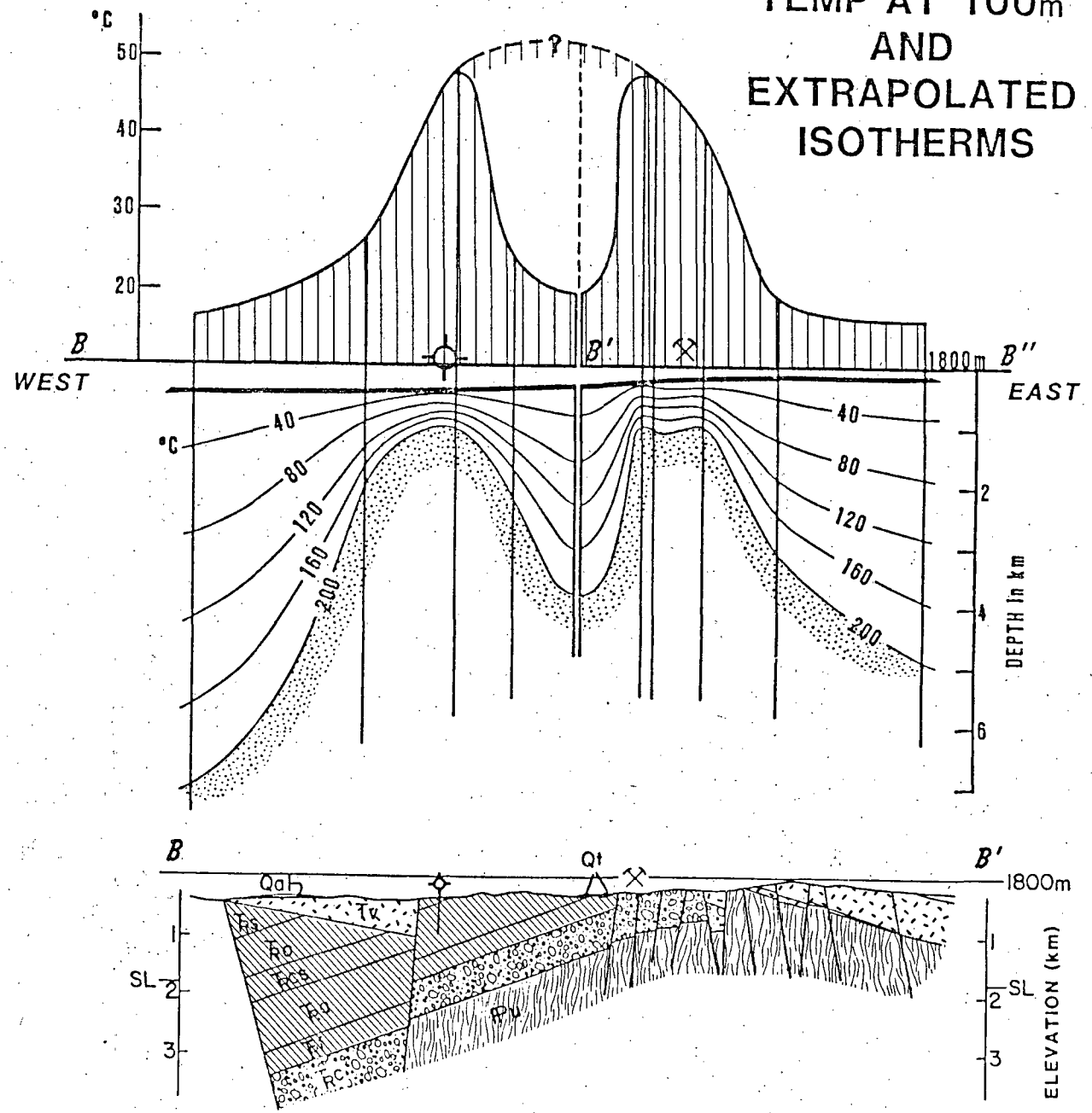


5R. Partial Landsat image showing the ring in center surrounding the McCoy prospect. Hole in the Wall wash drains the ring and empties into Dixie Valley on the west



6L
 Simplified geologic map, showing locations of McCoy and Wildhorse mines. PP, Permo-Pennsylvanian sediments; TRJ, Triassic-Jurassic conglomerates, carbonates and sandstones; T, Tertiary volcanics; Qal, Quaternary alluvium; Qt, Quaternary hot spring travertines. (after Pilkington, 1979)

B-B'-B''
TEMP AT 100m
AND
EXTRAPOLATED
ISOTHERMS



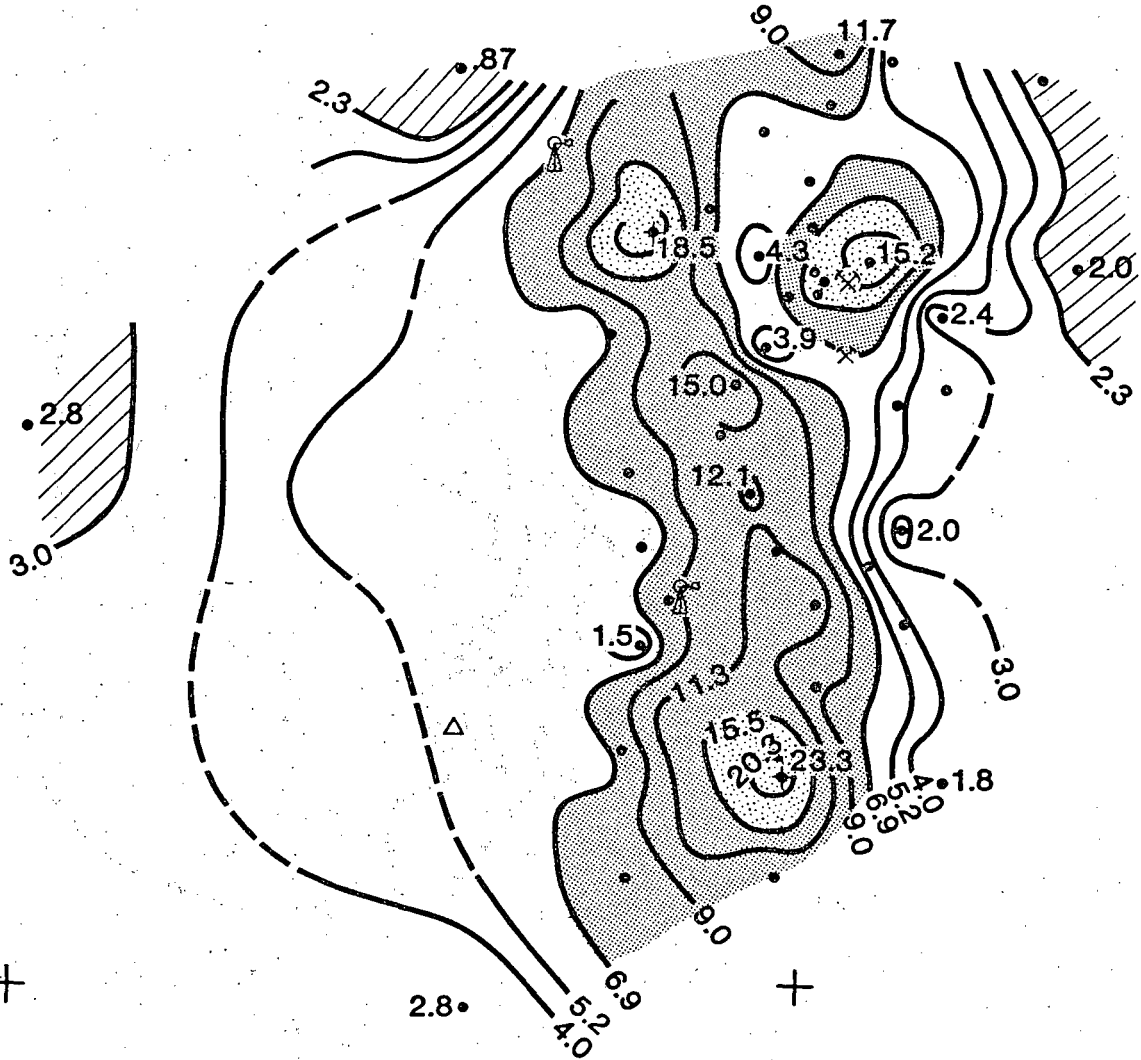
7R. East-west geologic profile through McCoy mine (See Slide 9L), with profile of temperature @ 100m and conductive isotherms

—117° 40'

—117° 30'

39° 55' +

+

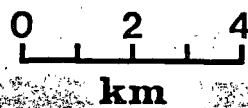


39° 45' +

+

HEAT FLOW (HFU)

• WELLS



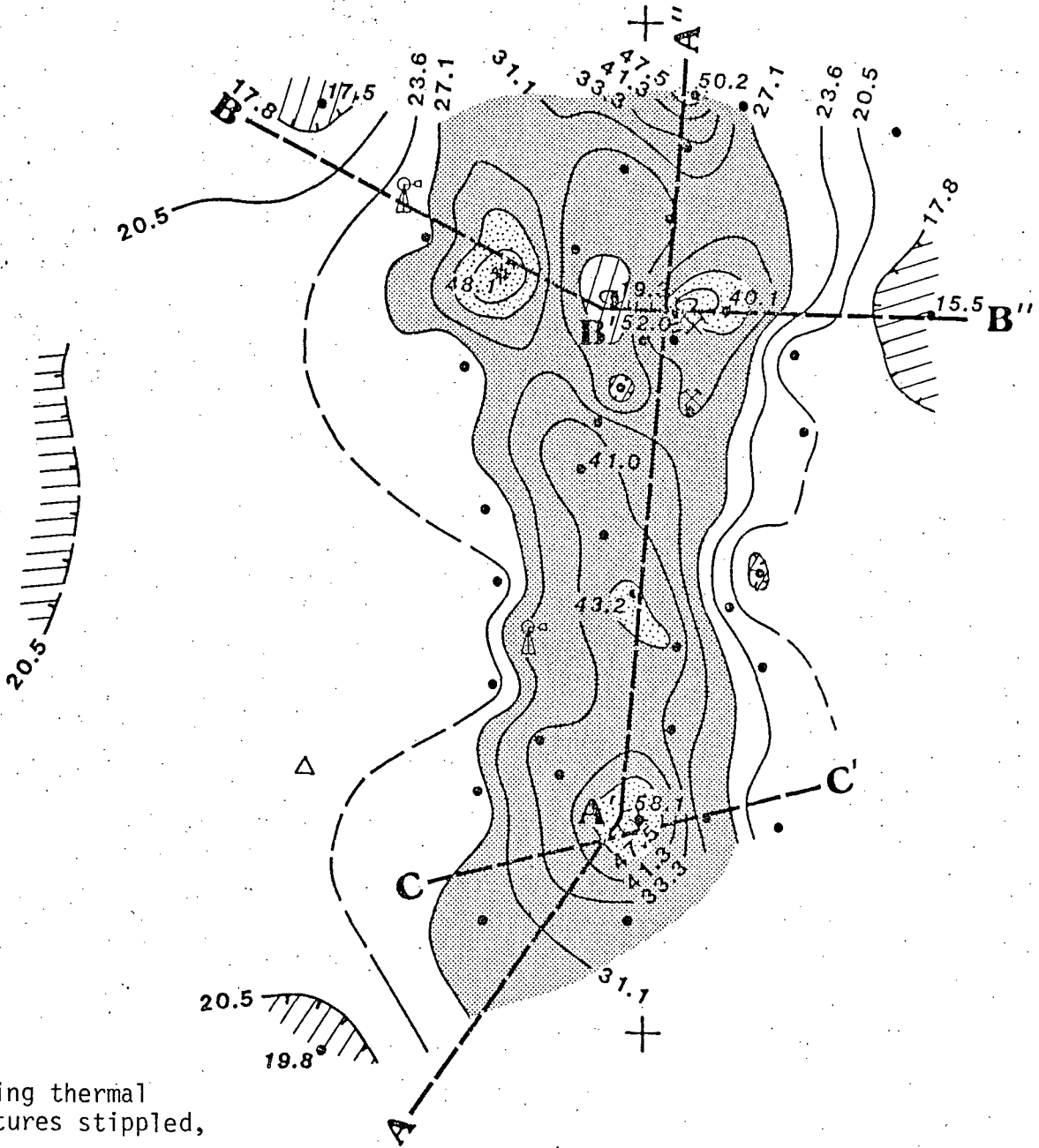
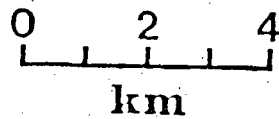
8L. Heatflow map showing thermal anomaly shaded, highest heatflows stippled and lowest, striped

39° 55' + 117° 40'

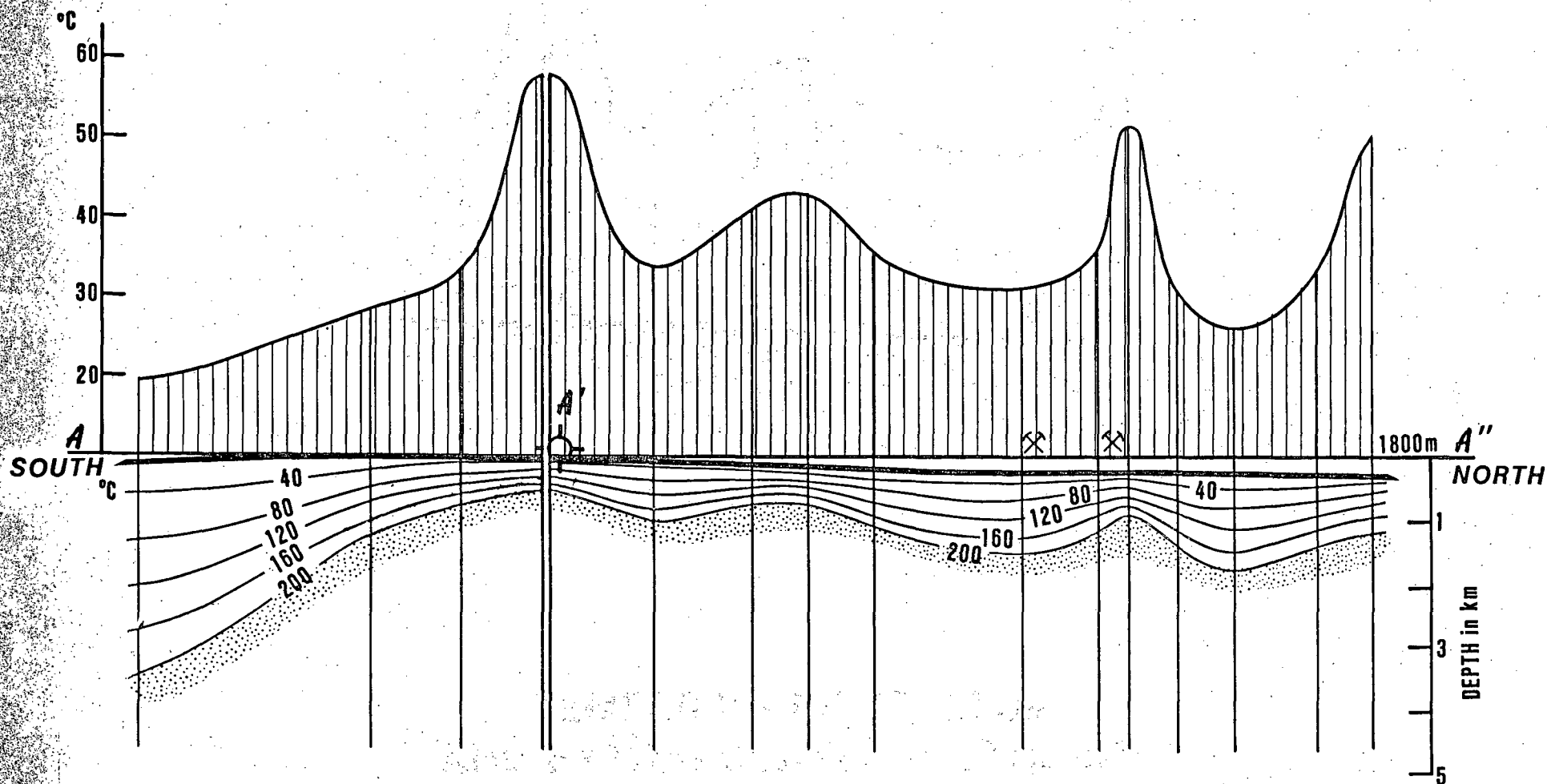
39° 45' +

TEMP. AT 100m (°C)

• WELLS

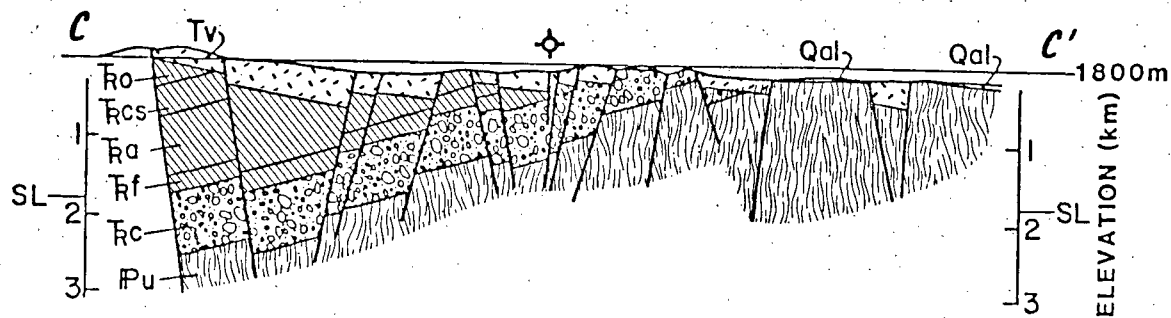
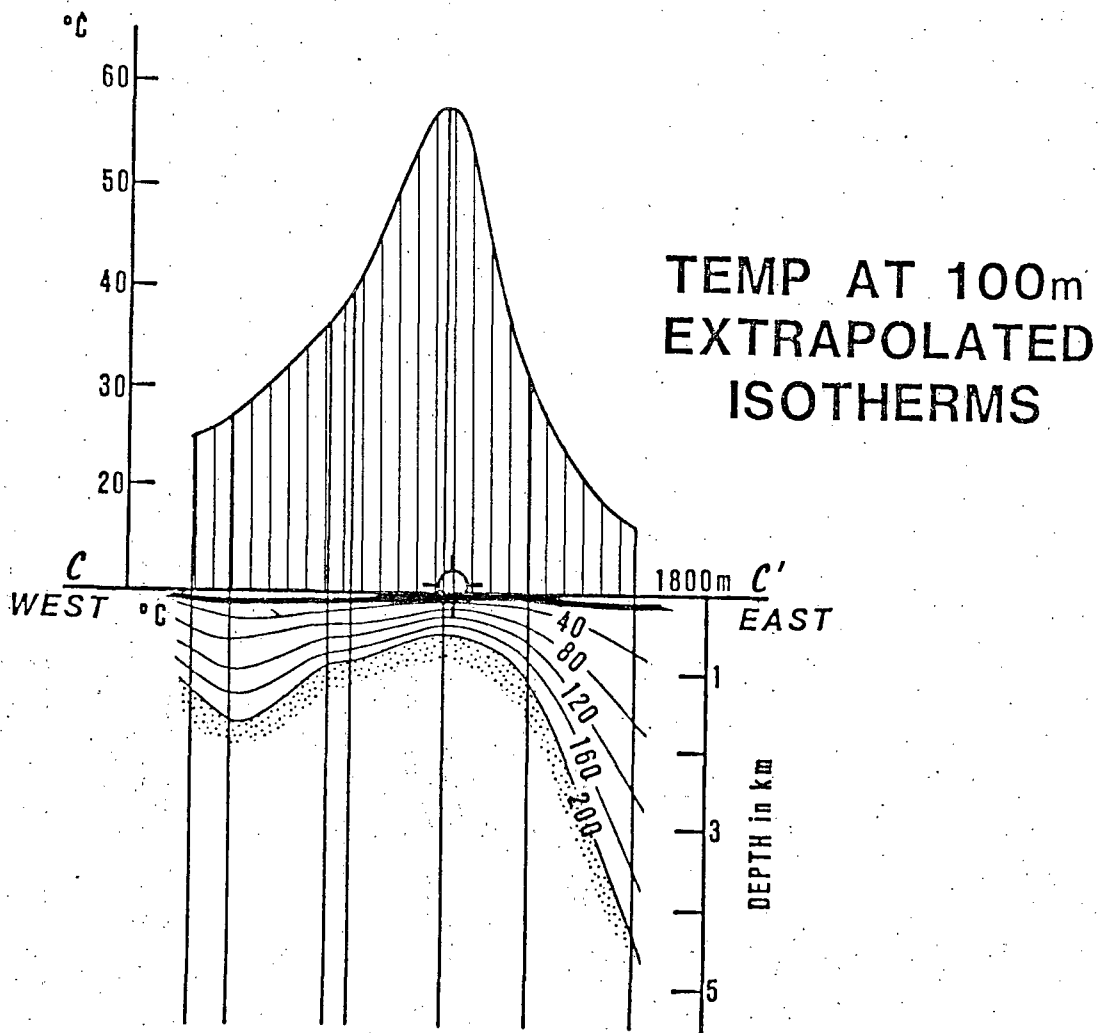


9L. Map of temperature at 100m showing thermal anomaly shaded, highest temperatures stippled, and lowest, striped

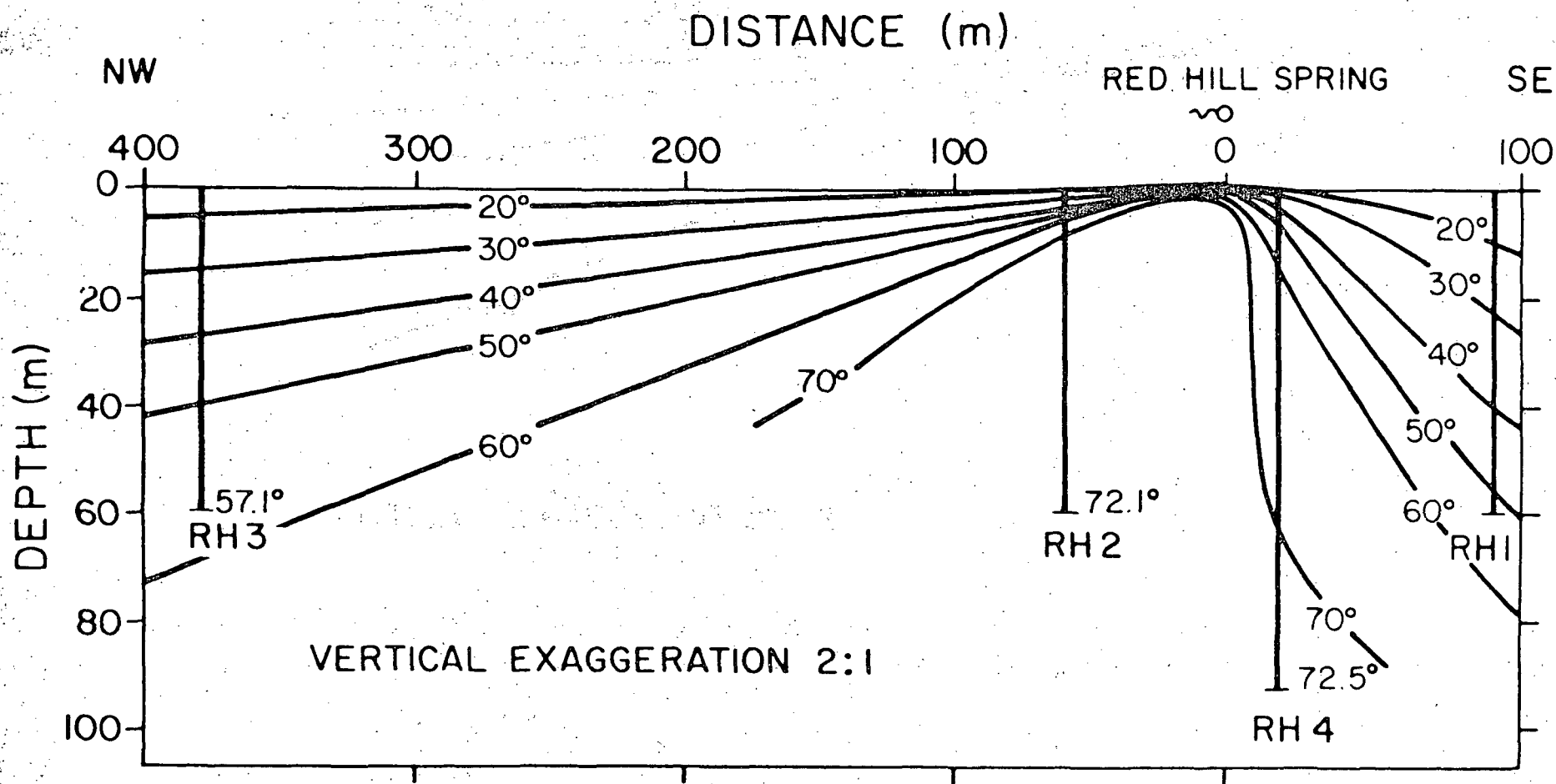


TEMPERATURE AT 100m AND EXTRAPOLATED ISOTHERMS

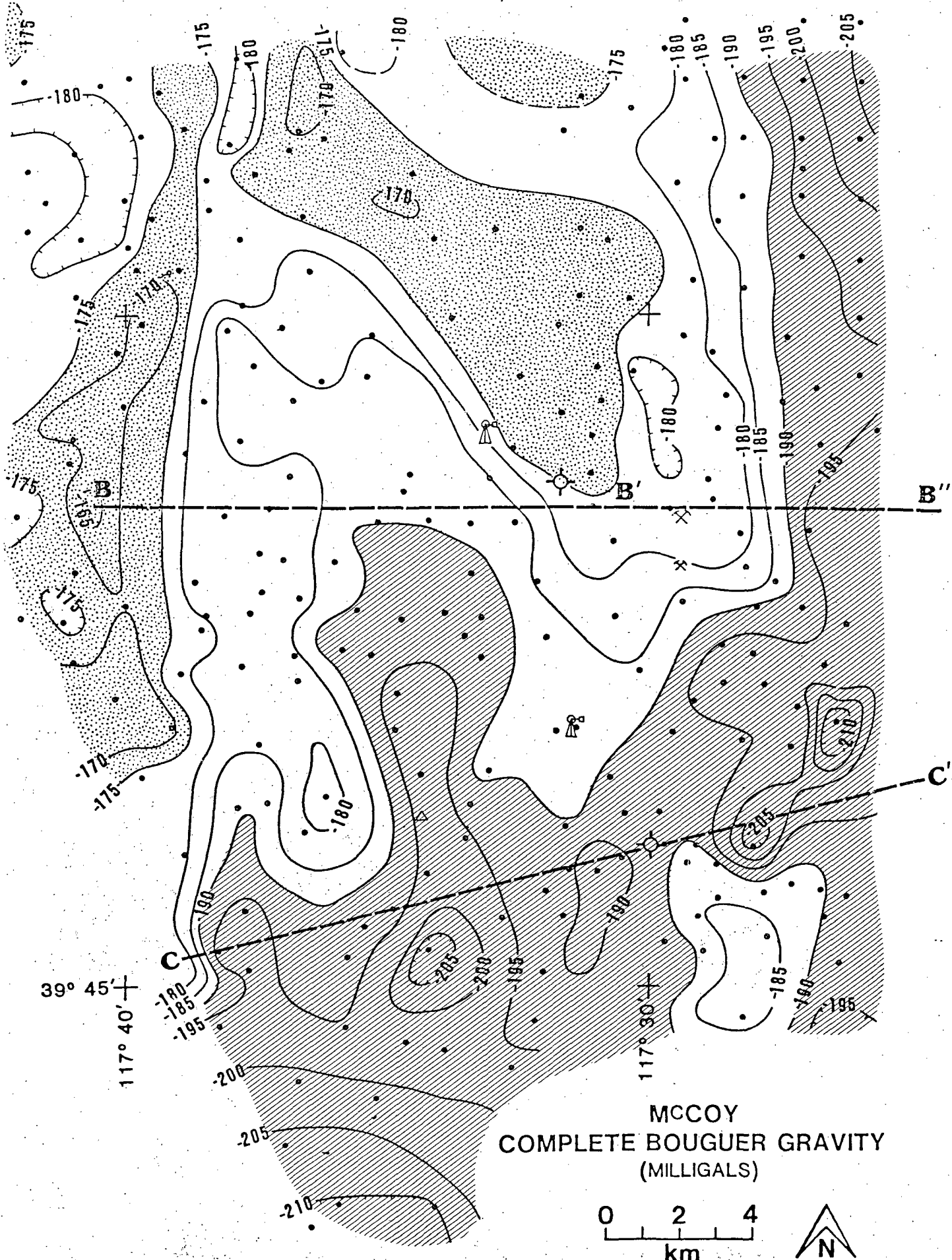
10R. Profile of temperatures and isotherms along Line A (N/S)



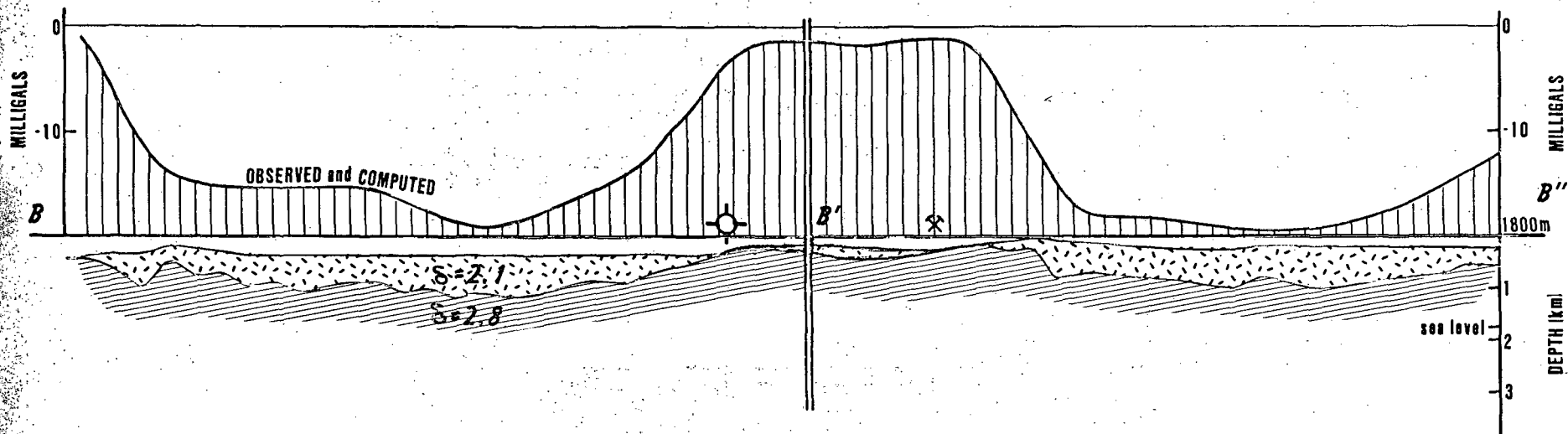
11R. Profile of temperatures and isotherms with geologic section along Line C (E/W) (Geology after Pilkington, 1979)



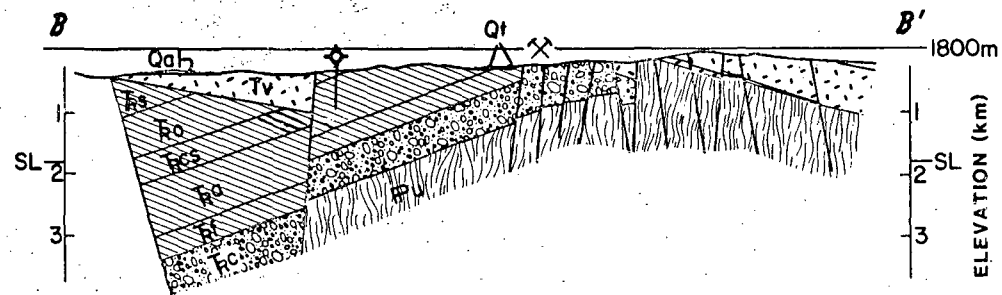
12L. Isothermal section at Red Hill Hot Spring, Utah, from Chapman, Kilty & Mase, 1978. Compare with Line C isotherms



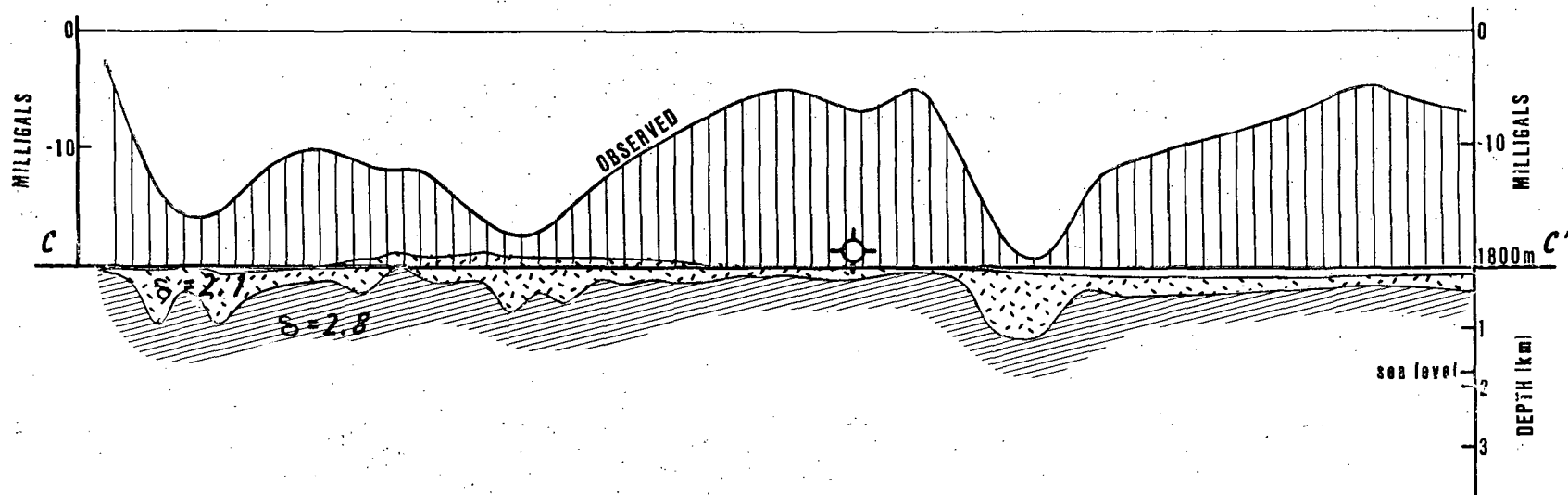
13L. Complete Bouguer gravity map. Highs are stippled; lows, striped



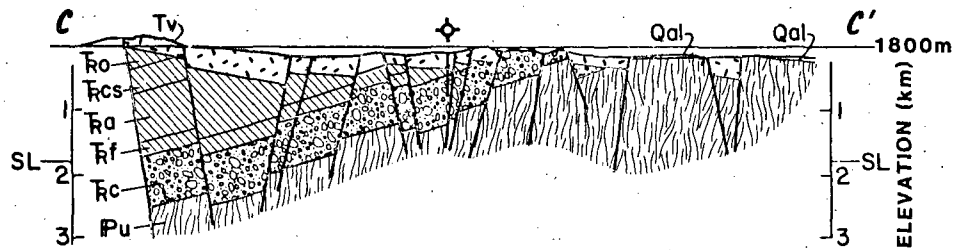
B-B'-B''
RESIDUAL GRAVITY
PROFILE
(COMPLETE BOUGUER)
AND DEPTH ANALYSIS



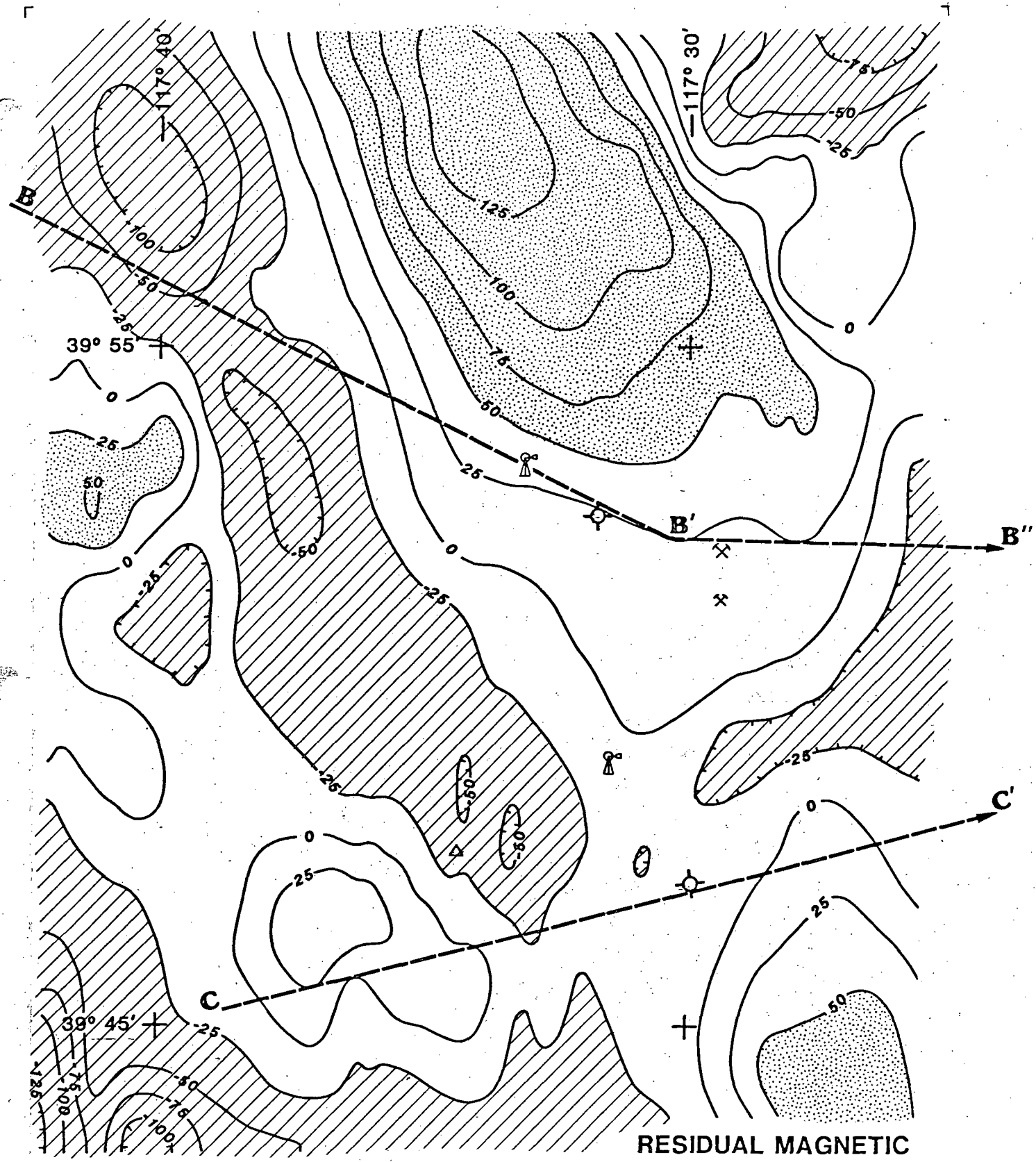
14R. Gravity profile, Line B, with automatic interpretation for densities 2.1 (checked) and 2.8gm/cm³ (striped)



C-C'
RESIDUAL GRAVITY
PROFILE
(COMPLETE BOUGUER)
AND DEPTH ANALYSIS

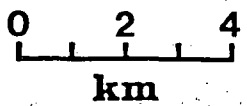


15R. Gravity profile, Line C, with automatic interpretation for densities 2.1 (checked) and 2.8gm/cm³ (striped)



RESIDUAL MAGNETIC INTENSITY

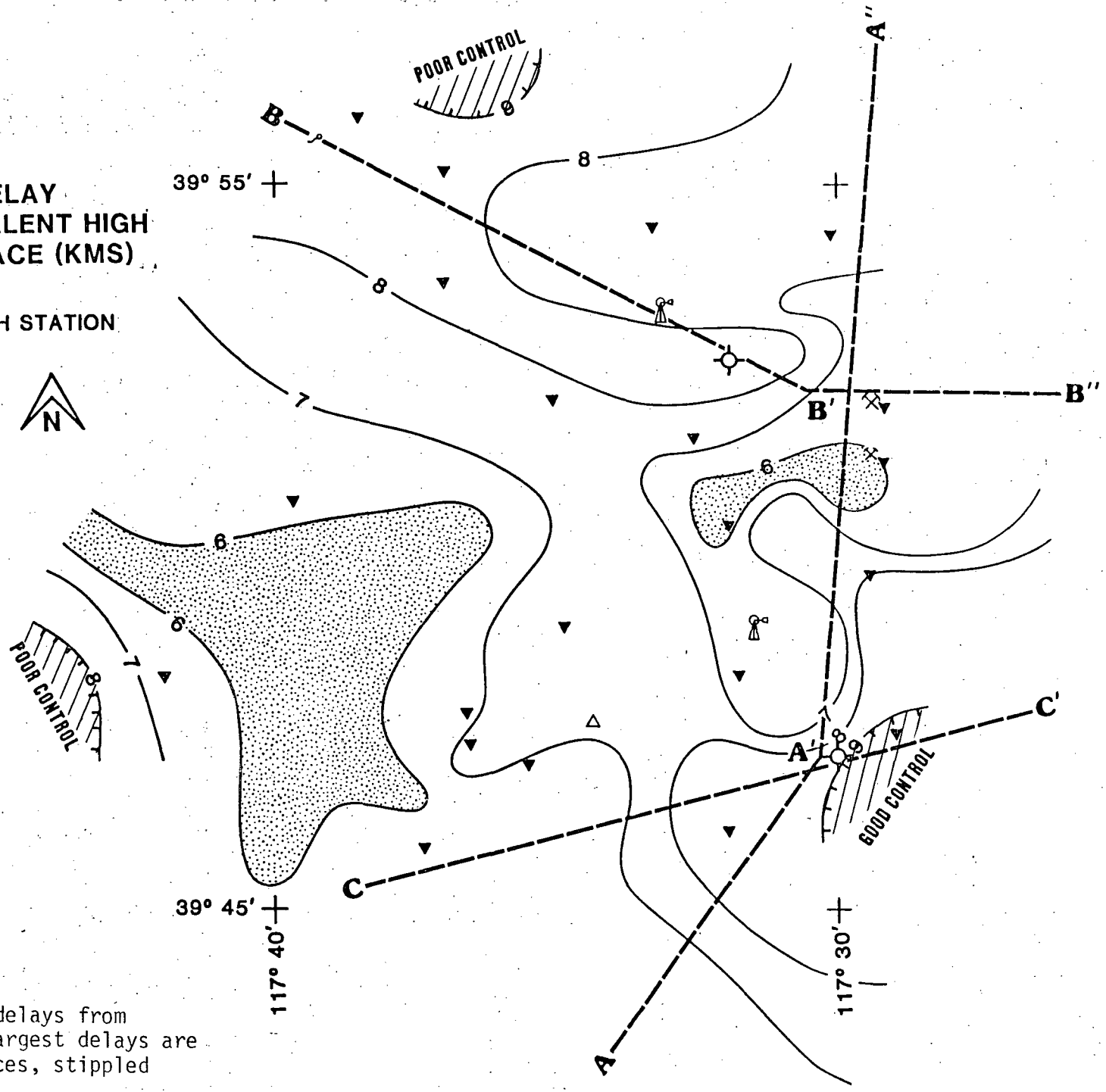
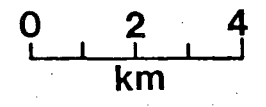
[gammas]



16L. Residual aeromagnetic map. Highs are stippled; lows, striped

**P-WAVE DELAY
DEPTH TO EQUIVALENT HIGH
VELOCITY SURFACE (KMS)**

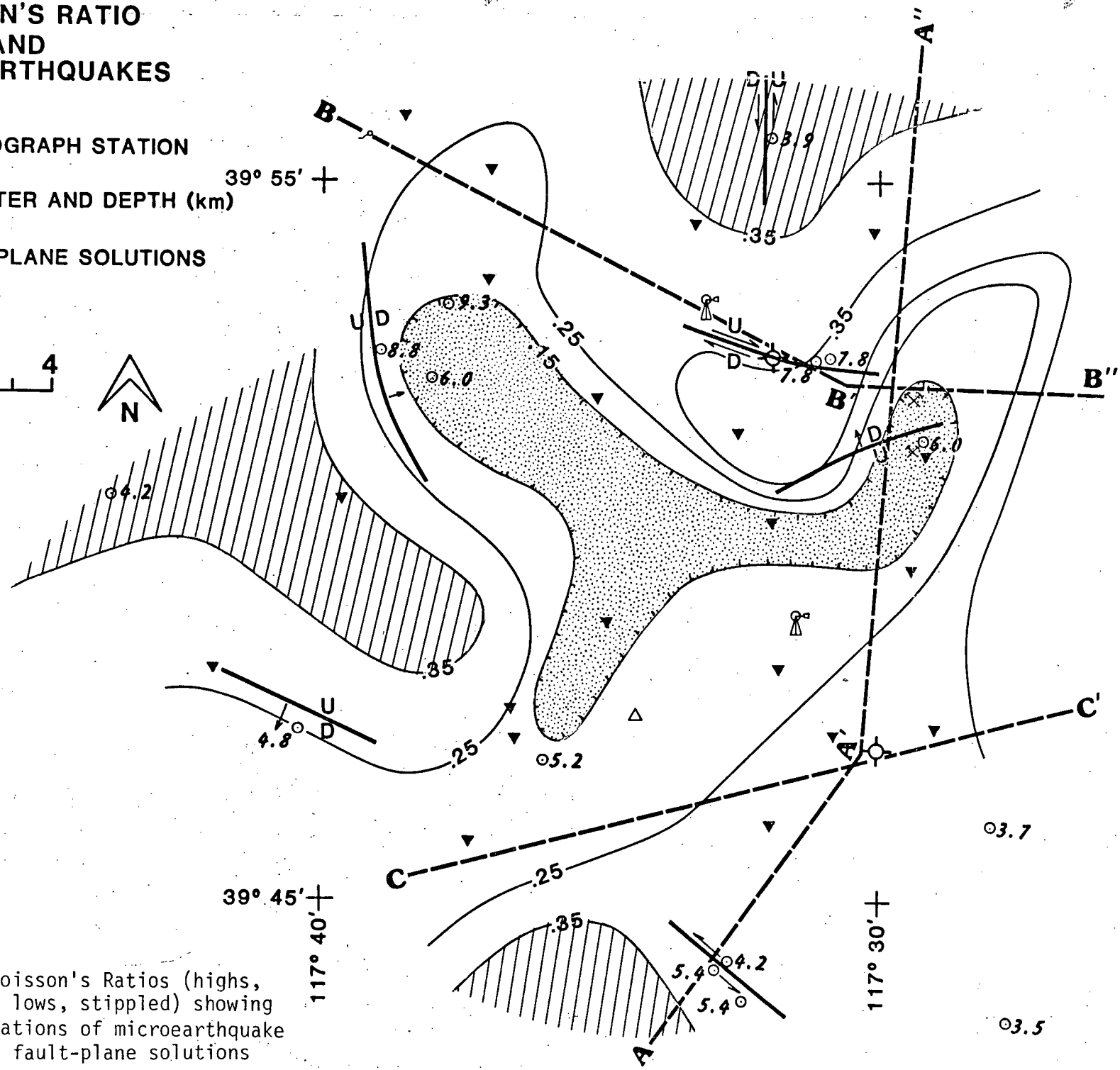
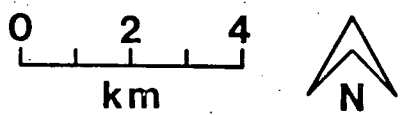
▼ SEISMOGRAPH STATION



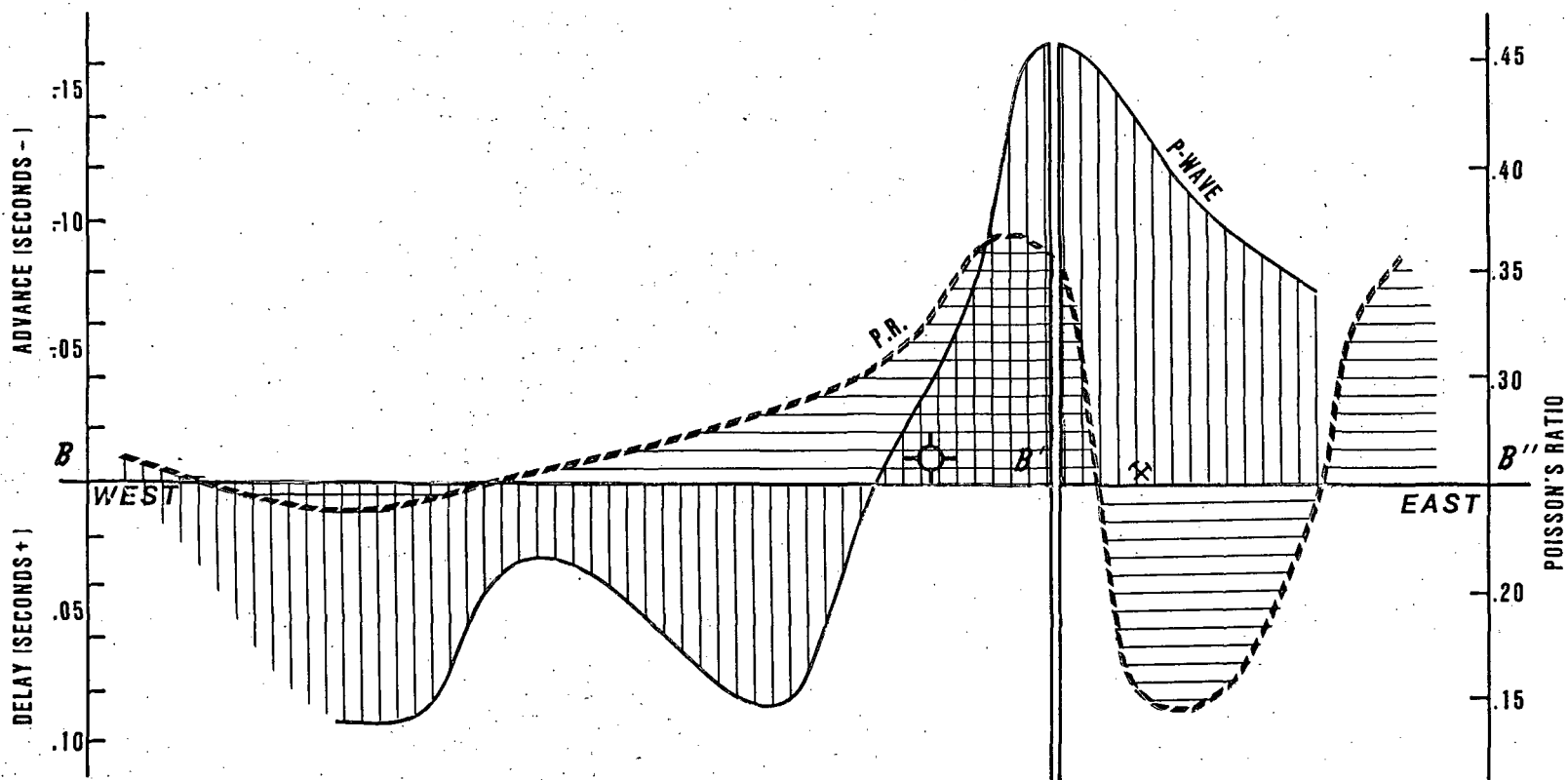
17R. Map of P-wave delays from teleseisms. Largest delays are striped; advances, stippled

POISSON'S RATIO AND MICROEARTHQUAKES

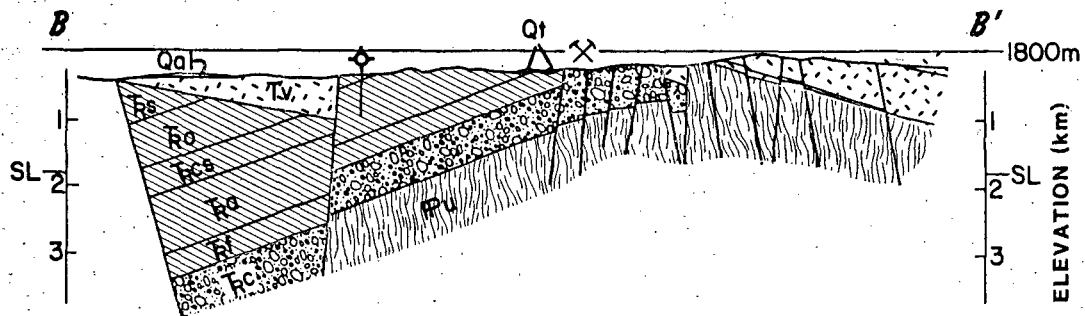
▼ SEISMOGRAPH STATION
 ○ 6.9 EPICENTER AND DEPTH (km)
 ↗ FAULT PLANE SOLUTIONS



18L. Map of Poisson's Ratios (highs, striped; lows, stippled) showing also locations of microearthquake foci and fault-plane solutions

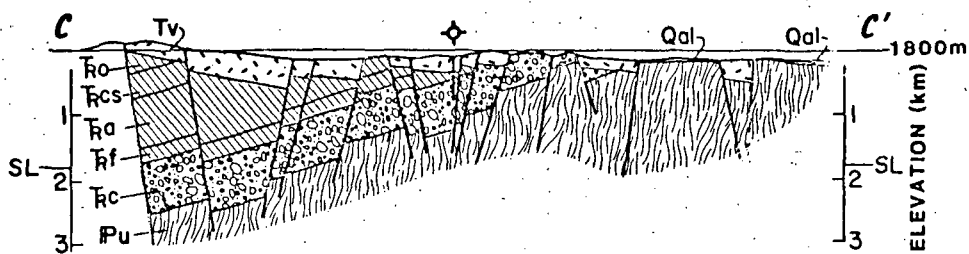
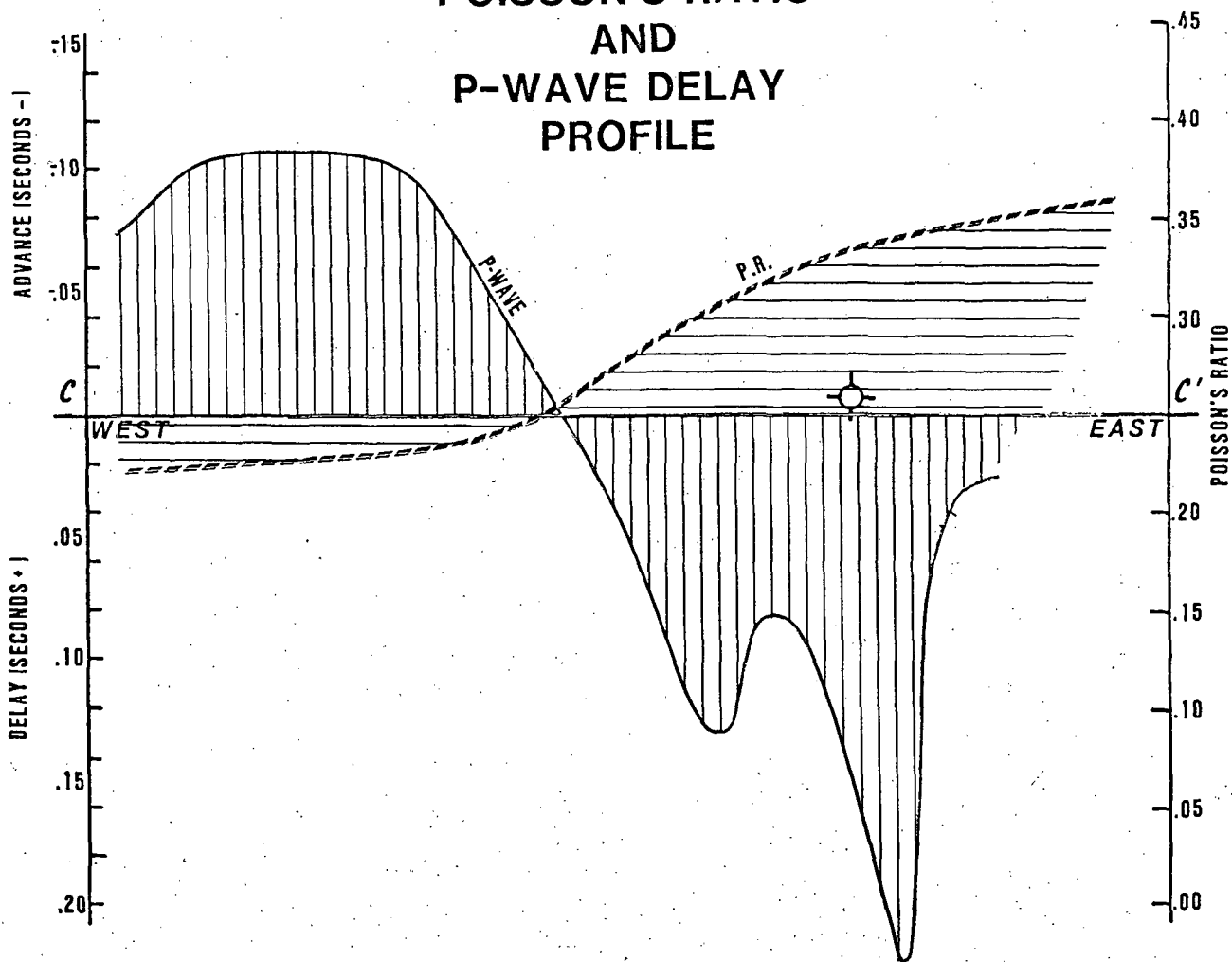


**B-B'-B''
POISSON'S RATIO
AND
P-WAVE DELAY
PROFILE**

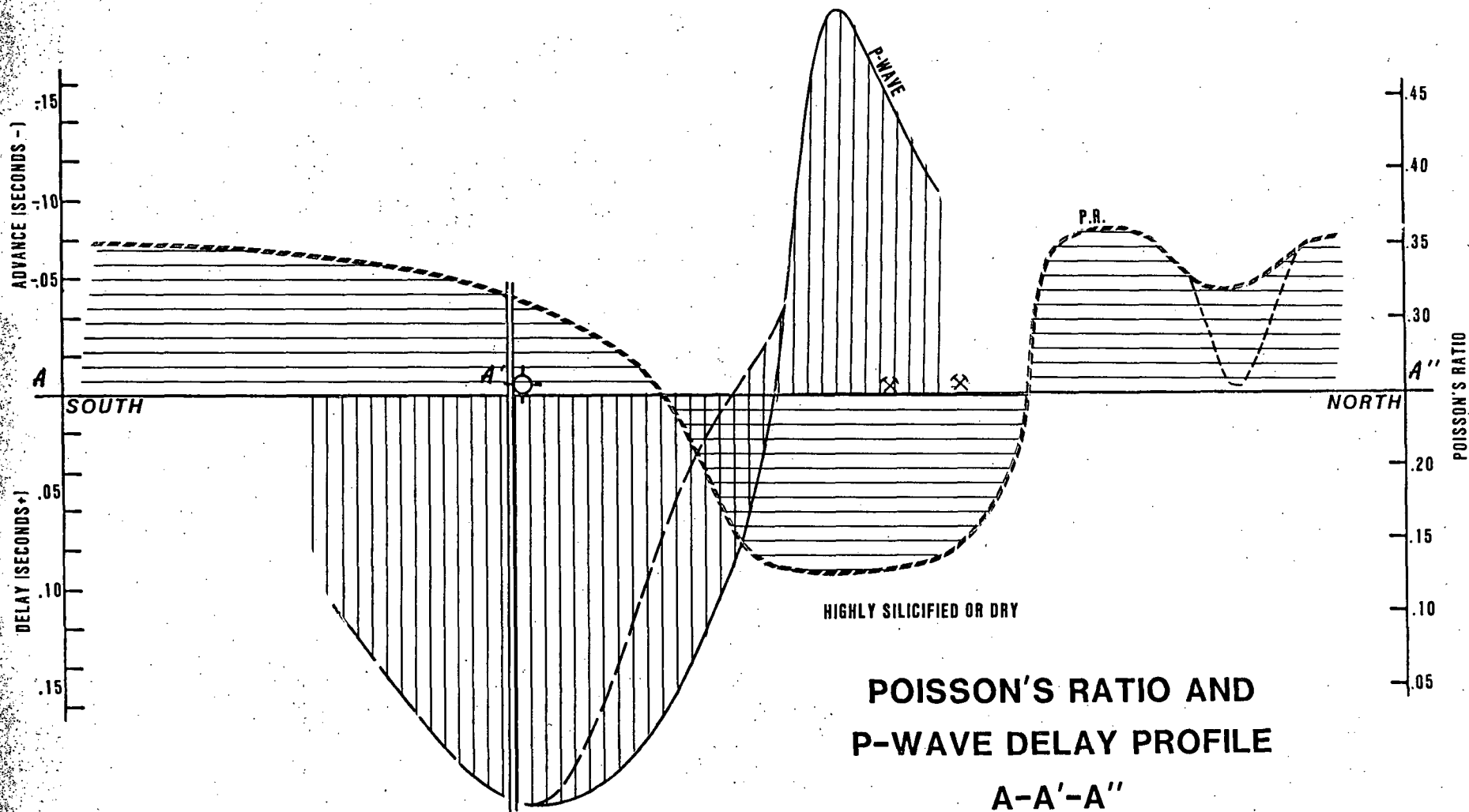


19R. Profiles of P-wave delays and advances and Poisson's Ratios along Line B

C-C' POISSON'S RATIO AND P-WAVE DELAY PROFILE



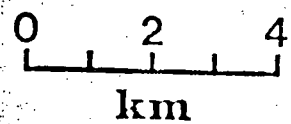
20R. Profiles of P-wave delays and advances and Poisson's Ratios along Line C



21R. Profiles of P-wave delays and advances and Poisson's Ratios along Line A

SELF POTENTIAL
(millivolts)

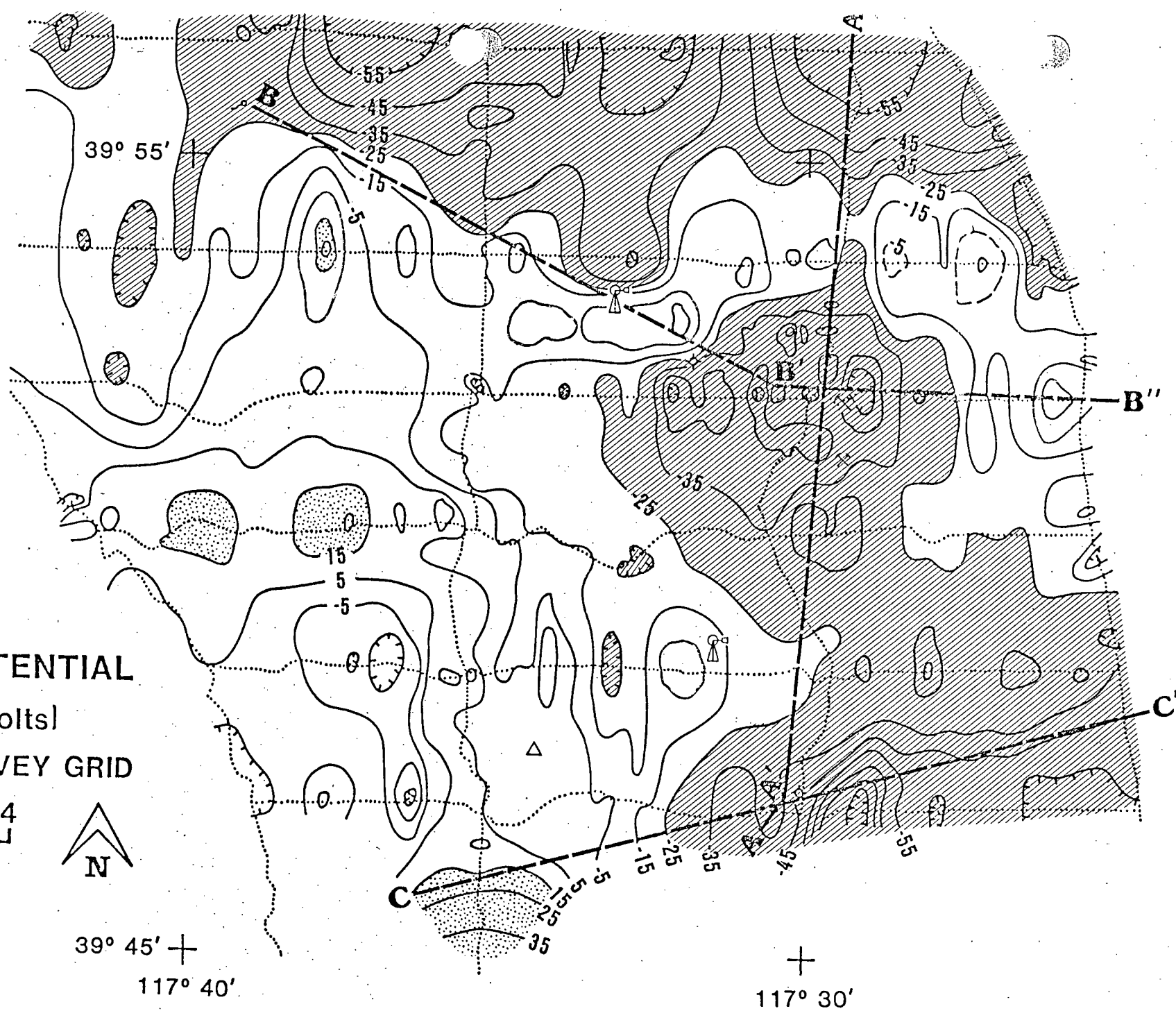
..... SURVEY GRID

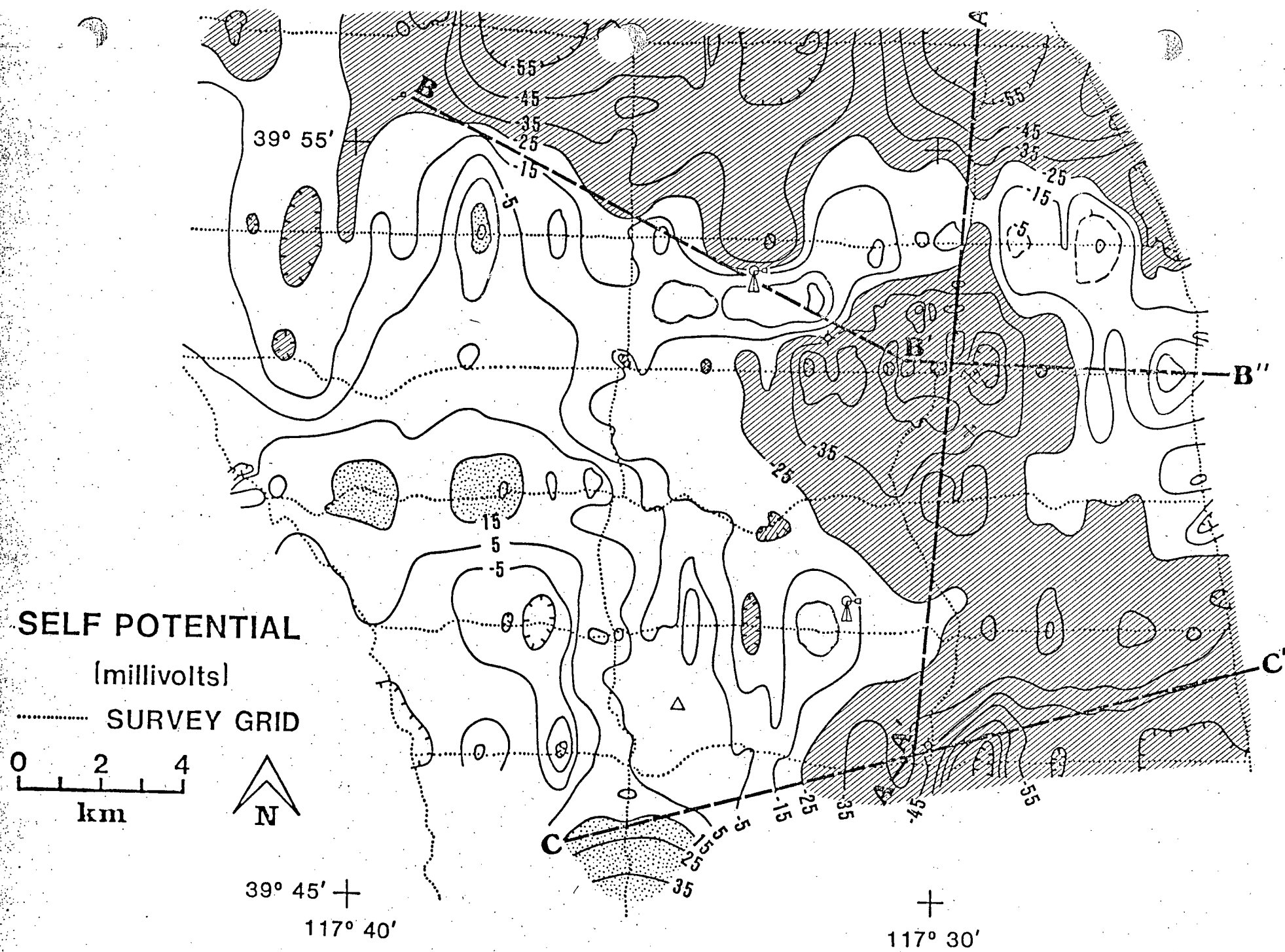


39° 45' +
117° 40'

+
117° 30'

22L. Map of self-potential response. Negatives are striped; highs stippled



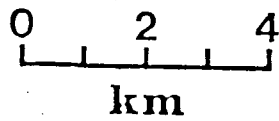


22L. Map of self-potential response. Negatives are striped; highs stippled

39° 55' + 117° 40'

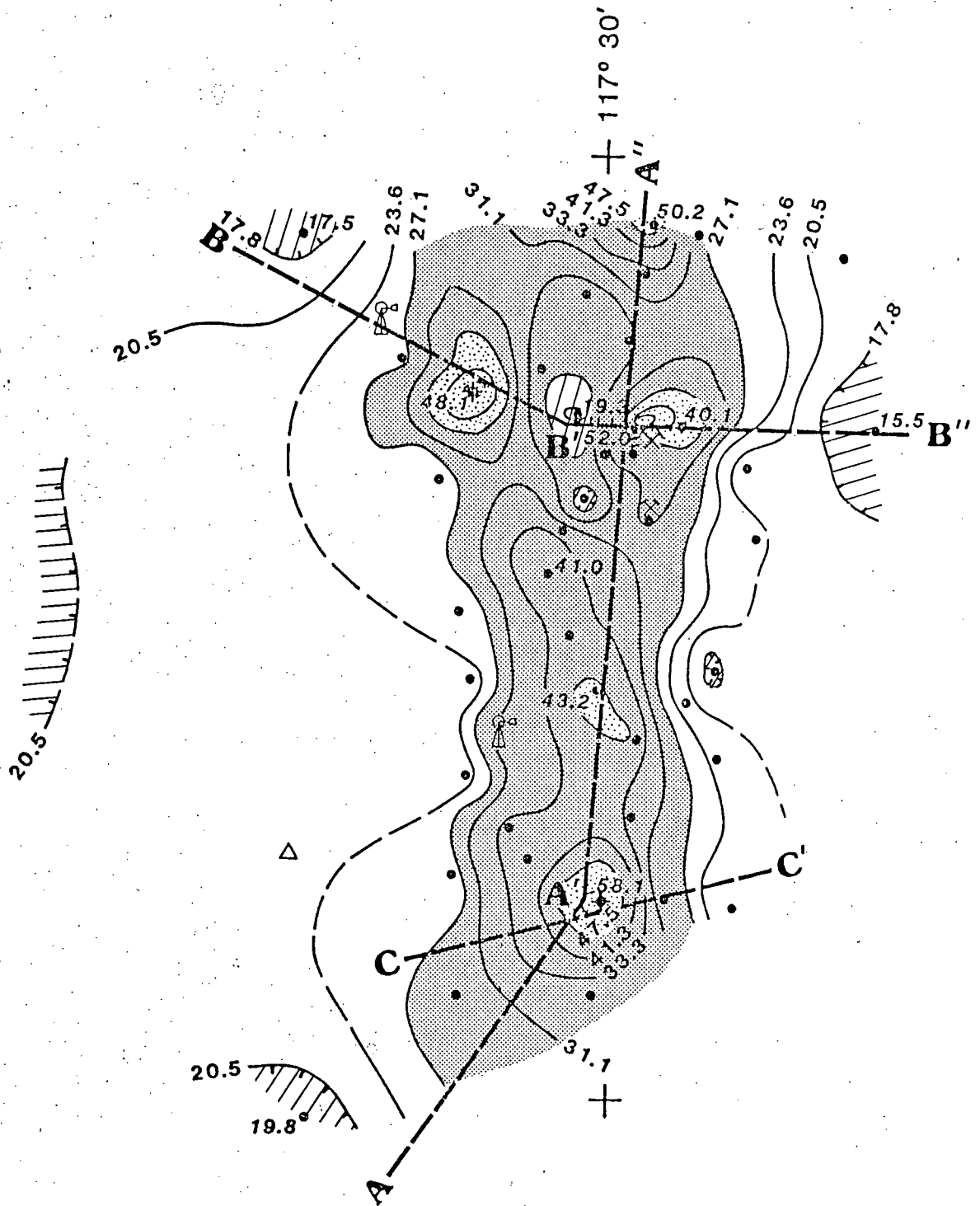
TEMP. AT 100m (C)

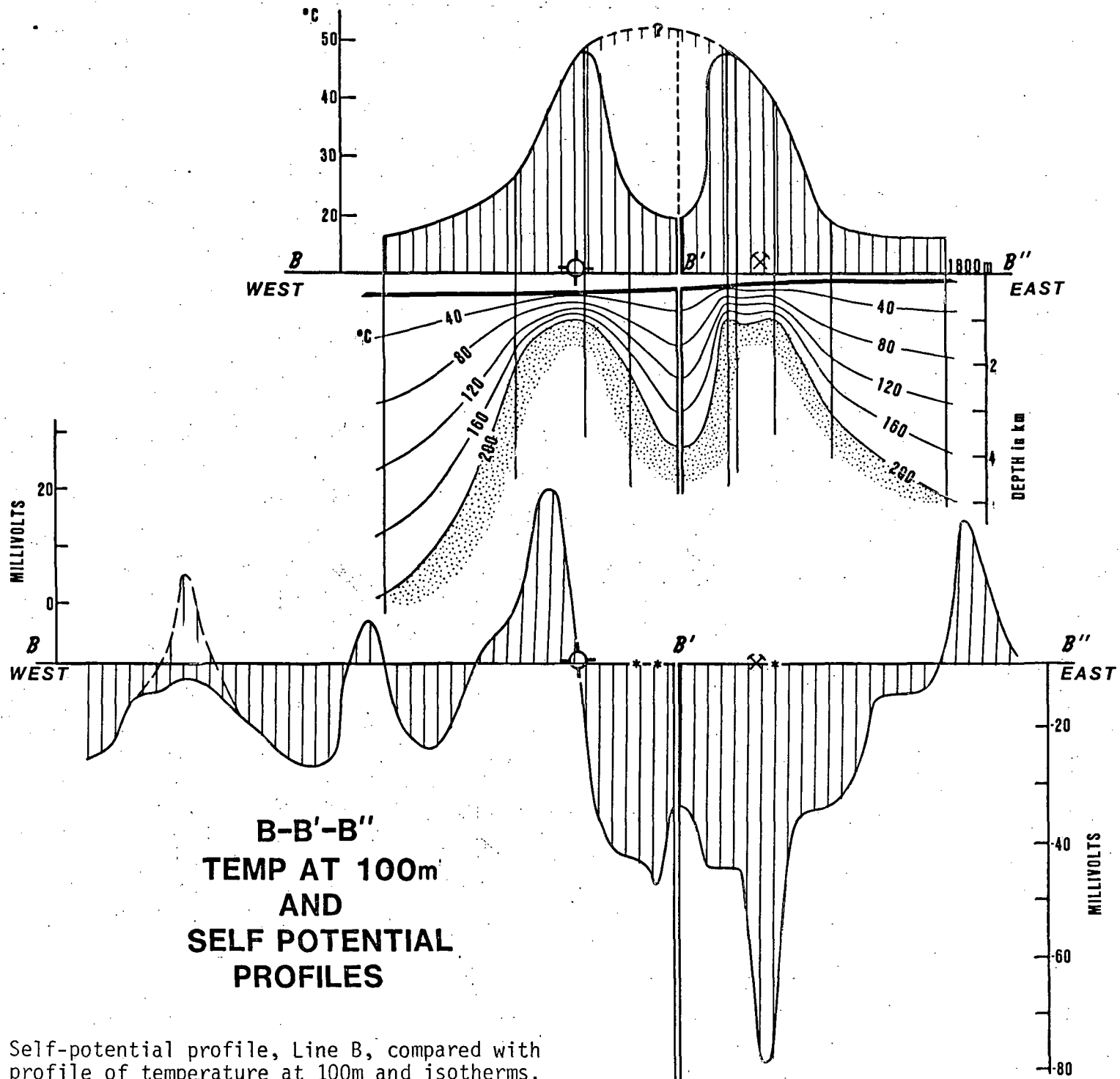
• WELLS



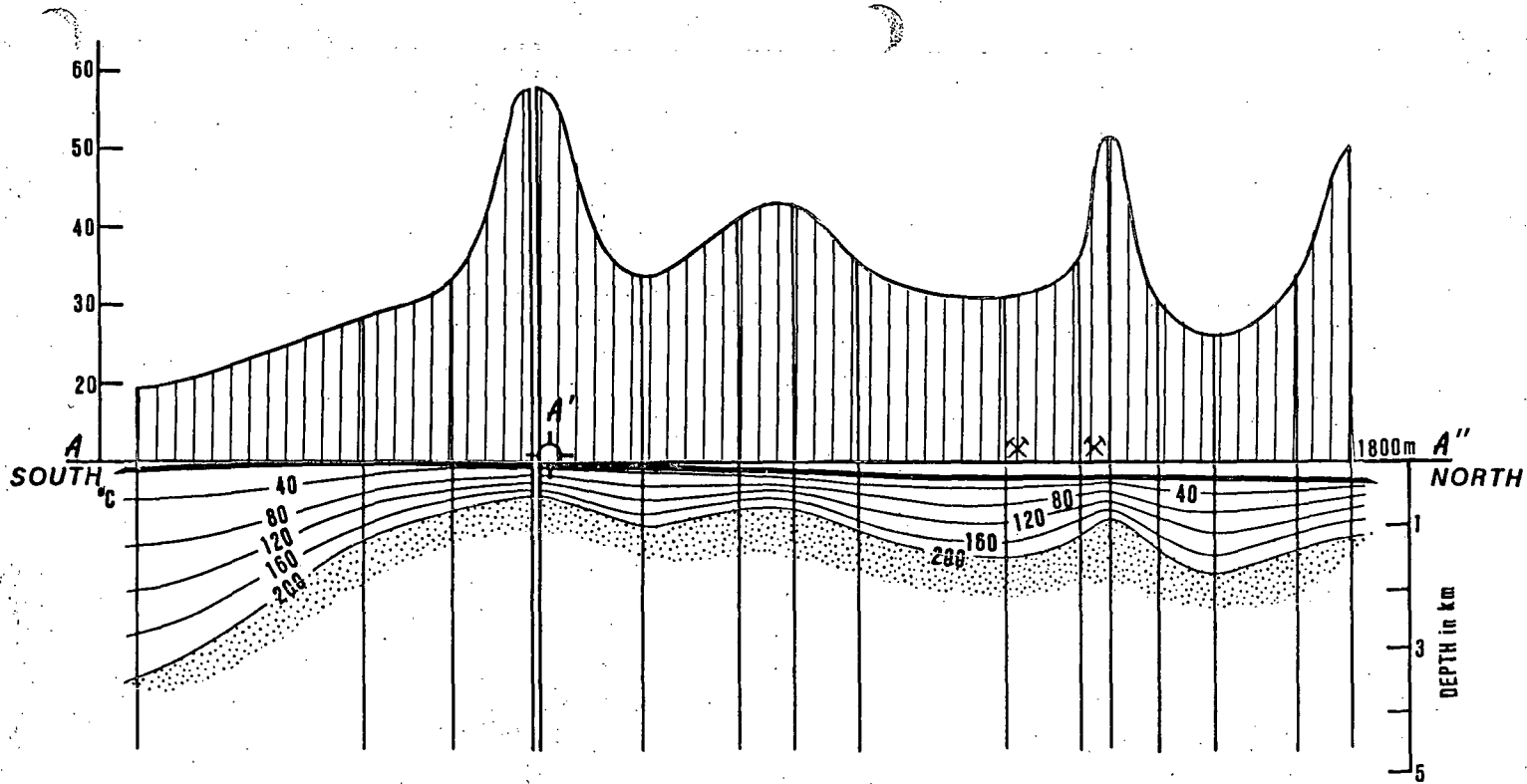
39° 45' +

23R. Refer to Figure 9L

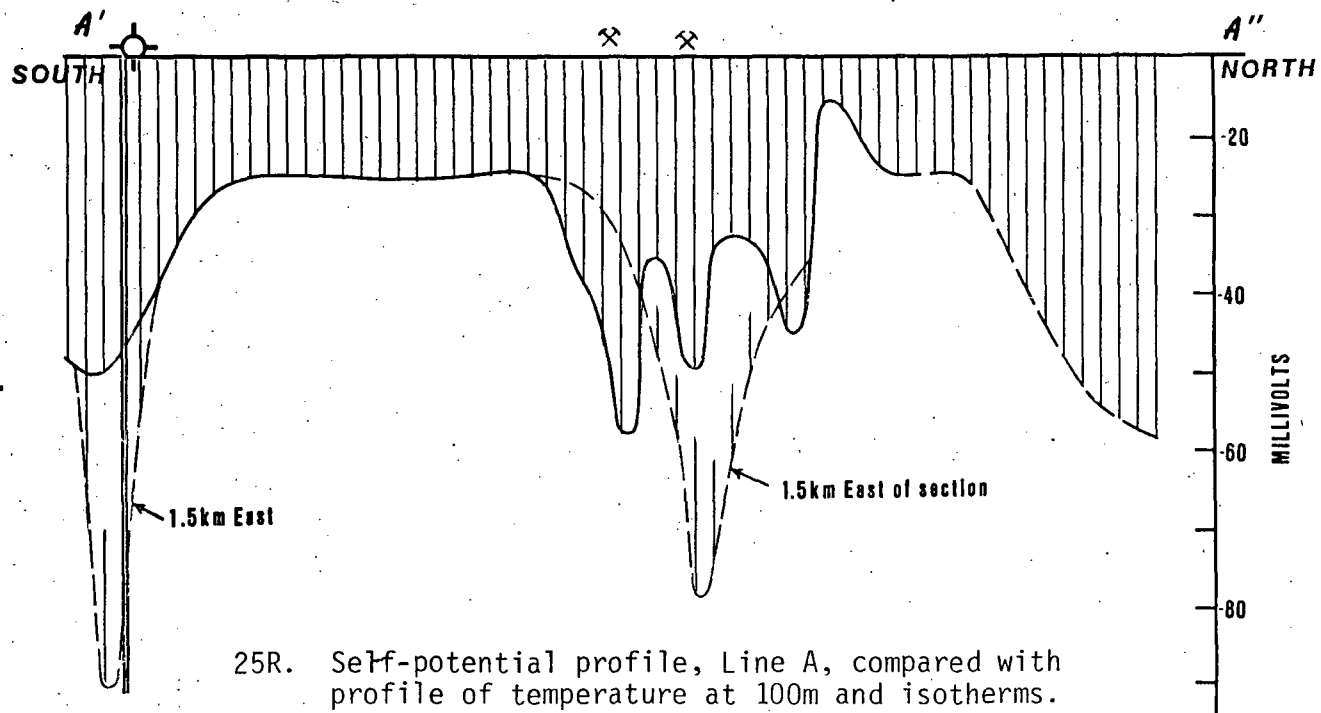




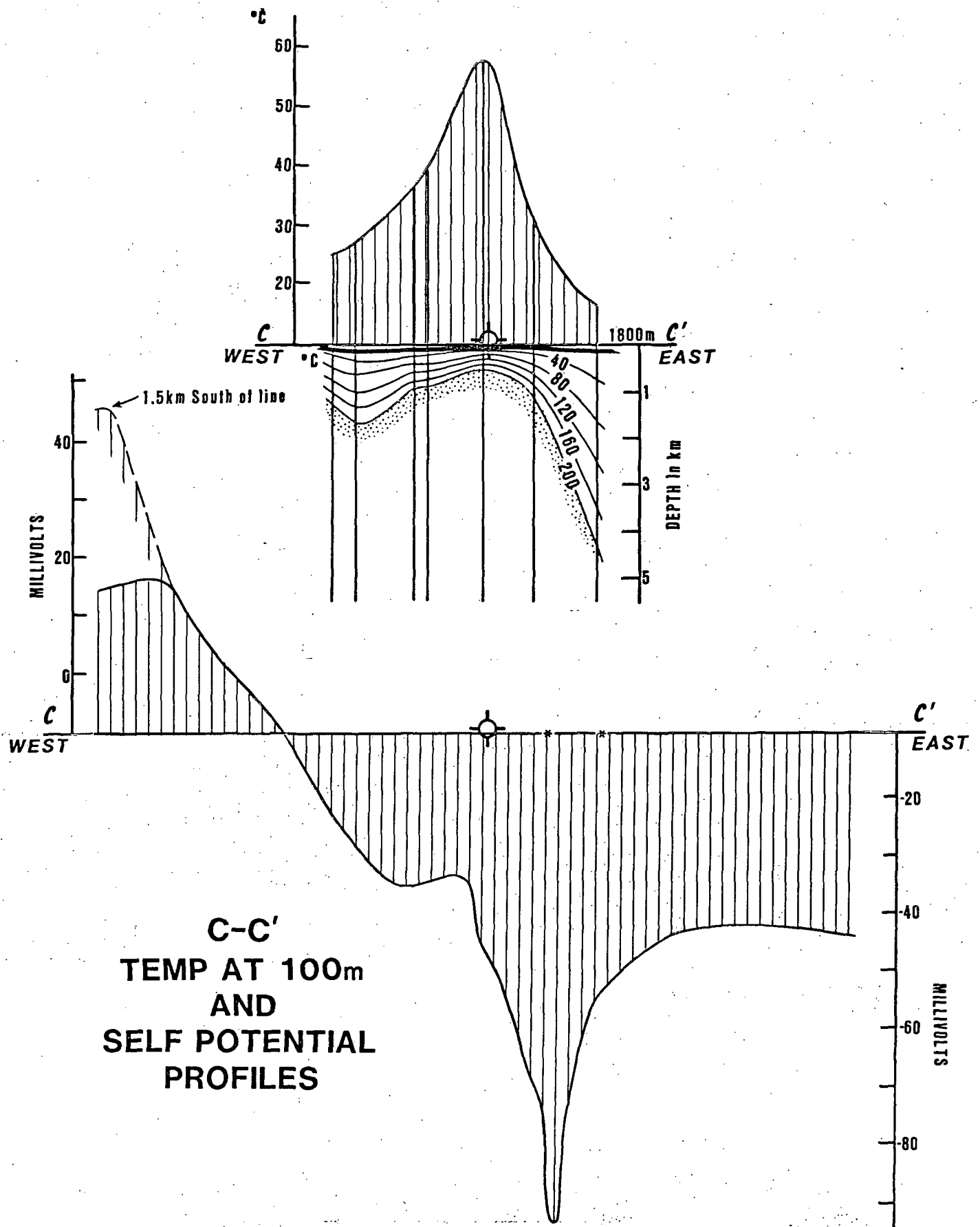
24R. Self-potential profile, Line B, compared with profile of temperature at 100m and isotherms. Microearthquake epicenters shown as stars



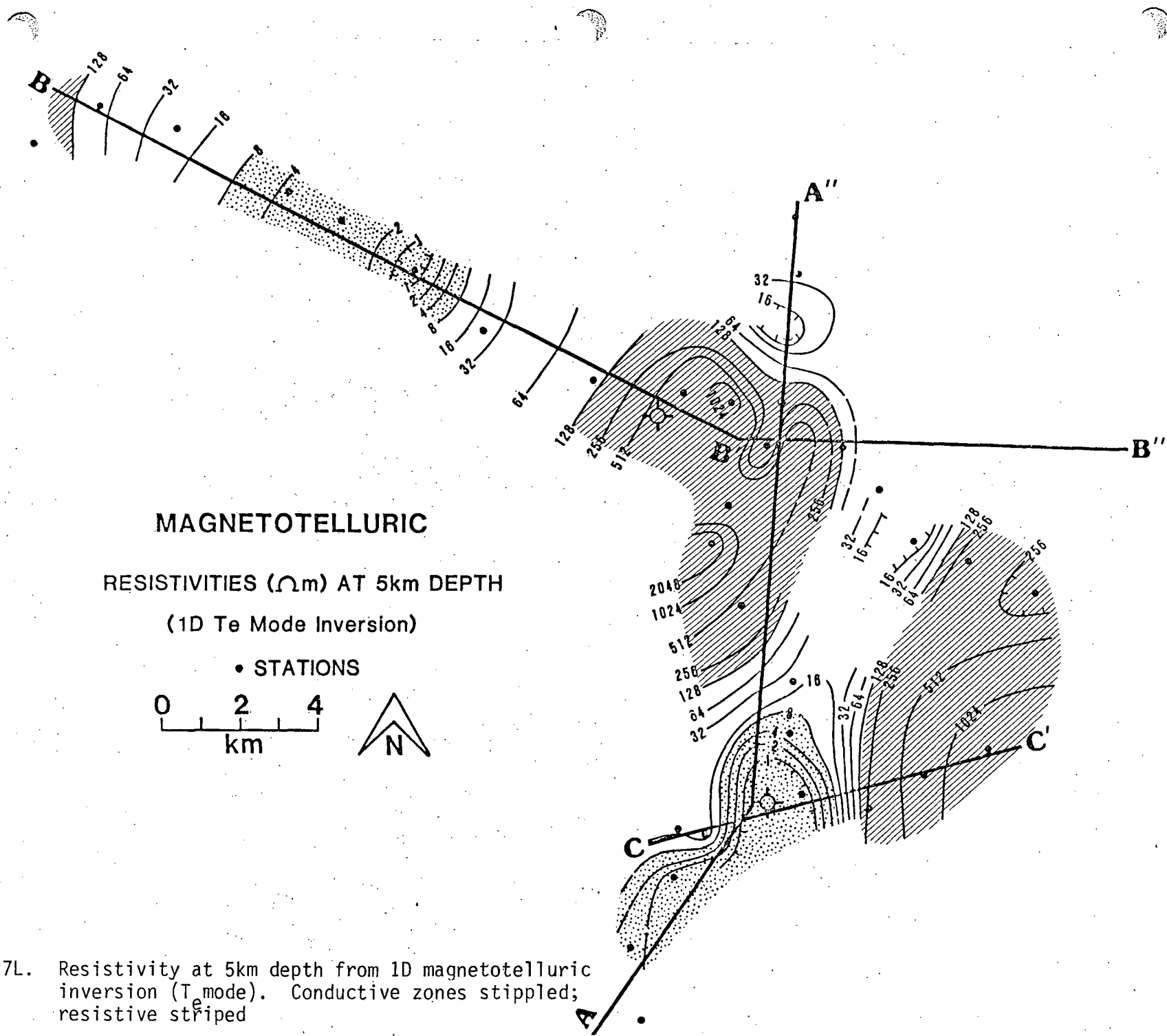
**A-A'-A''
TEMP AT 100m
AND
SELF POTENTIAL
PROFILES**



25R. Self-potential profile, Line A, compared with profile of temperature at 100m and isotherms. Microearthquake epicenters shown as stars



26R. Self-potential profile, Line C, compared with profile of temperature at 100m and isotherms. Microearthquake epicenters shown as stars

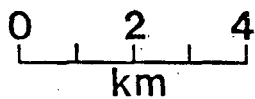


MAGNETOTELLURIC

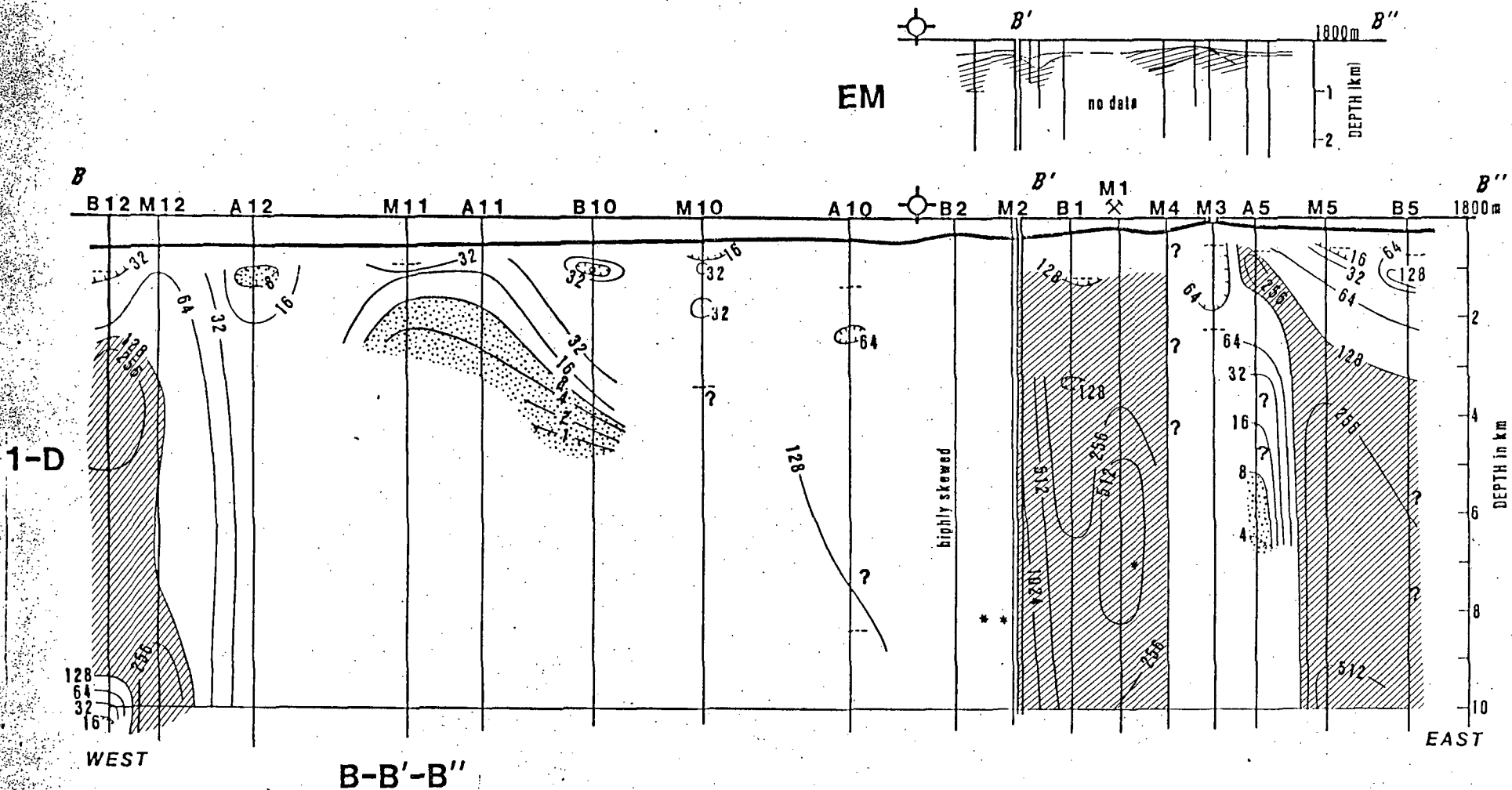
RESISTIVITIES (Ωm) AT 5km DEPTH

(1D Te Mode Inversion)

• STATIONS



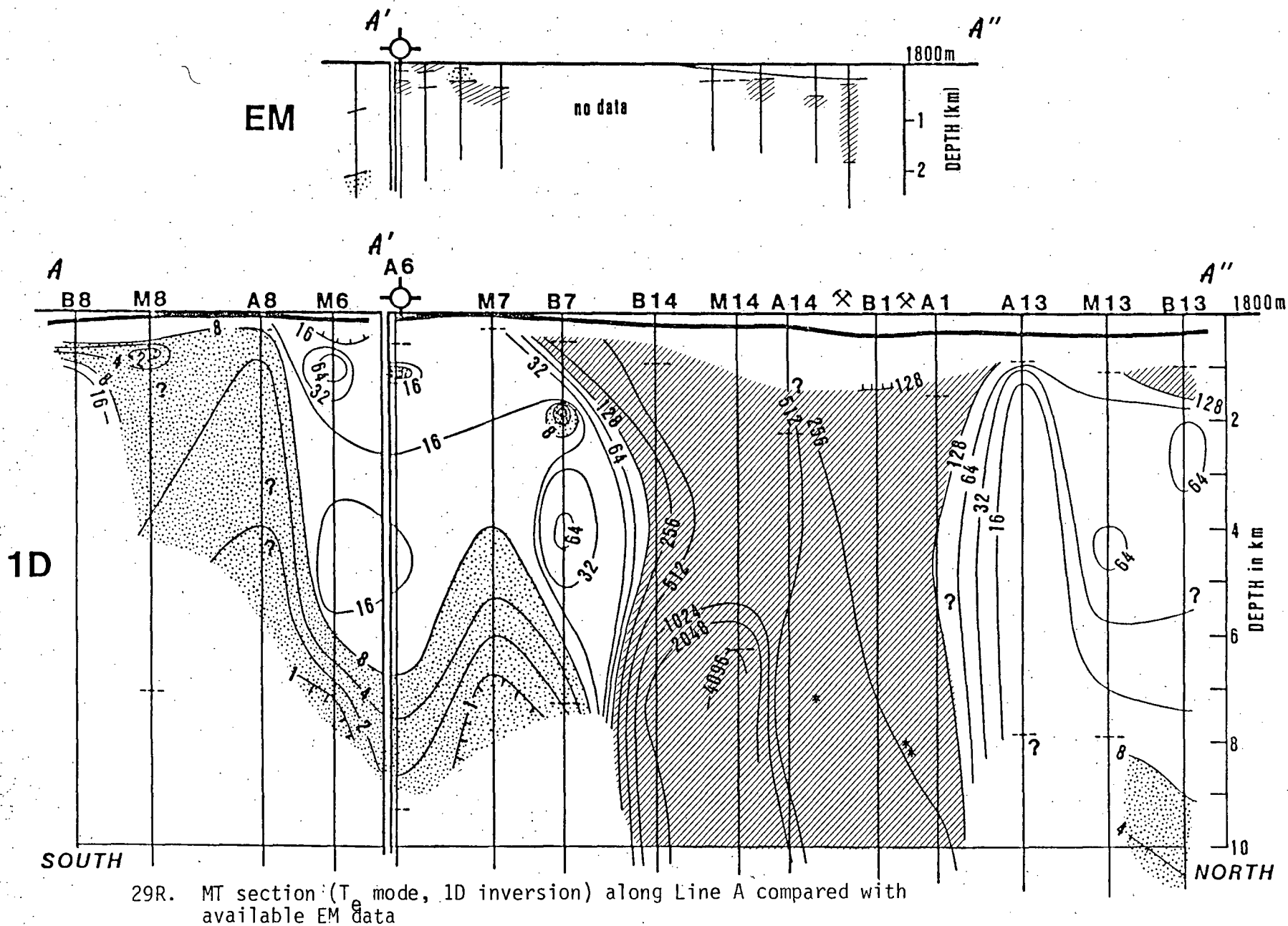
27L. Resistivity at 5km depth from 1D magnetotelluric inversion (T mode). Conductive zones stippled; resistive striped

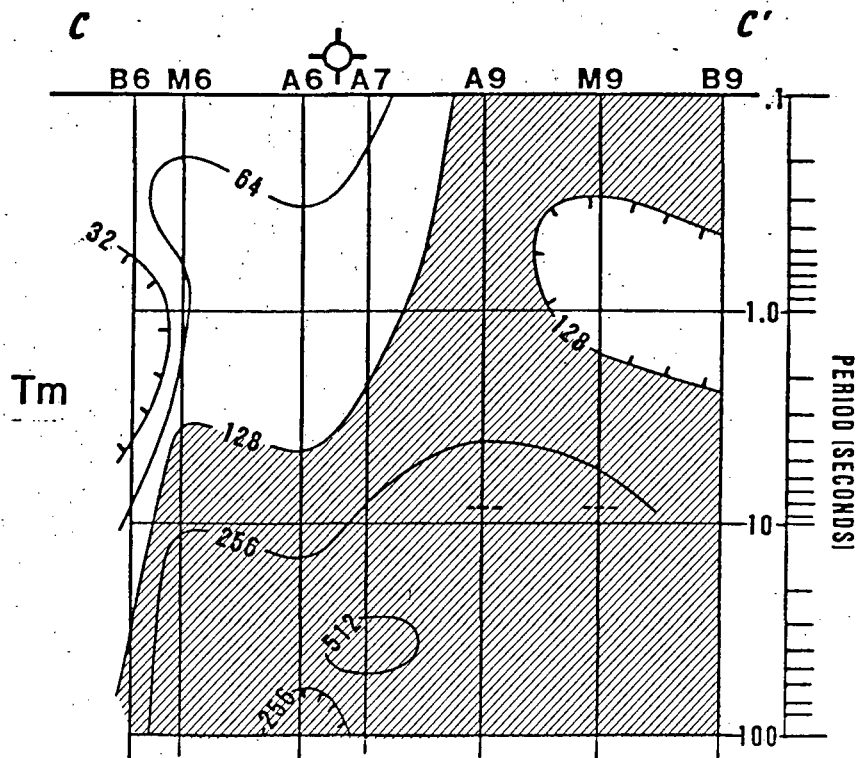
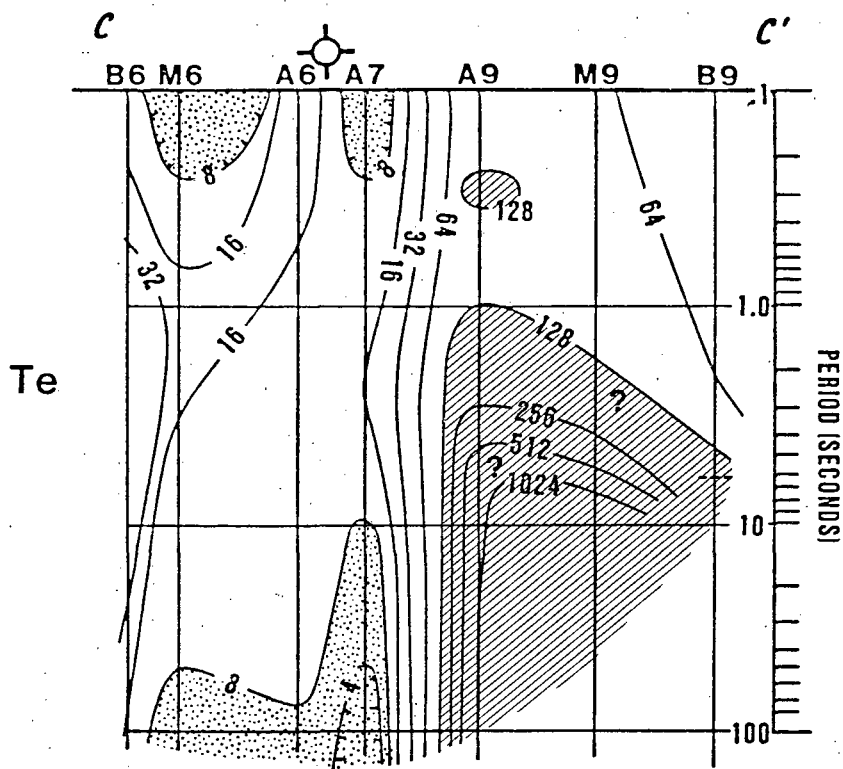


B-B'-B''
MAGNETOTELLURIC
1-D INVERSION WITH
EM AND GEOLOGIC PROFILES

28R. Magnetotelluric section (T_e mode, 1D inversion) along Line B compared with available EM^e section and geology

MAGNETOTELLURIC 1-D INVERSION WITH EM PROFILE A-A'-A''

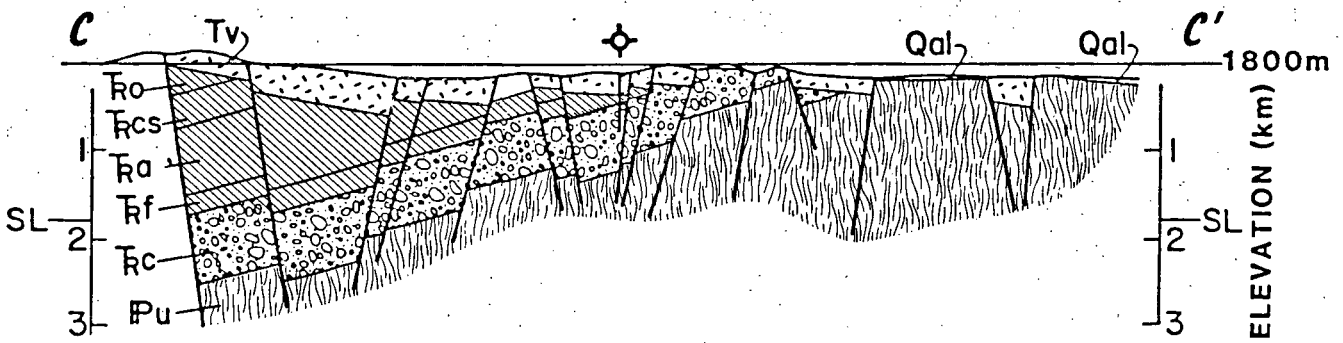
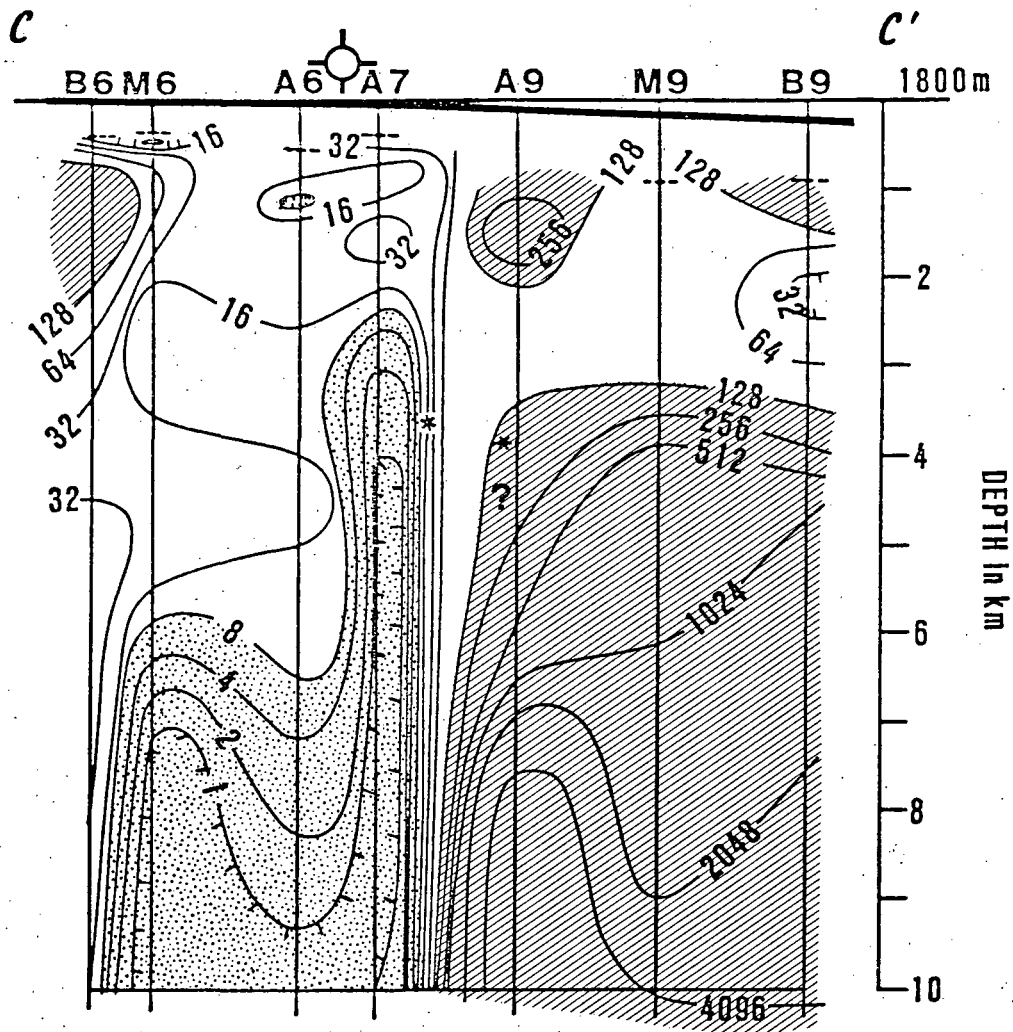




C-C'

MAGNETOTELLURIC PSEUDOSECTION

30R. MT pseudosections (resistivity vs. period) along Line C



C-C'

MAGNETOTELLURIC 1-D INVERSION WITH GEOLOGIC PROFILE

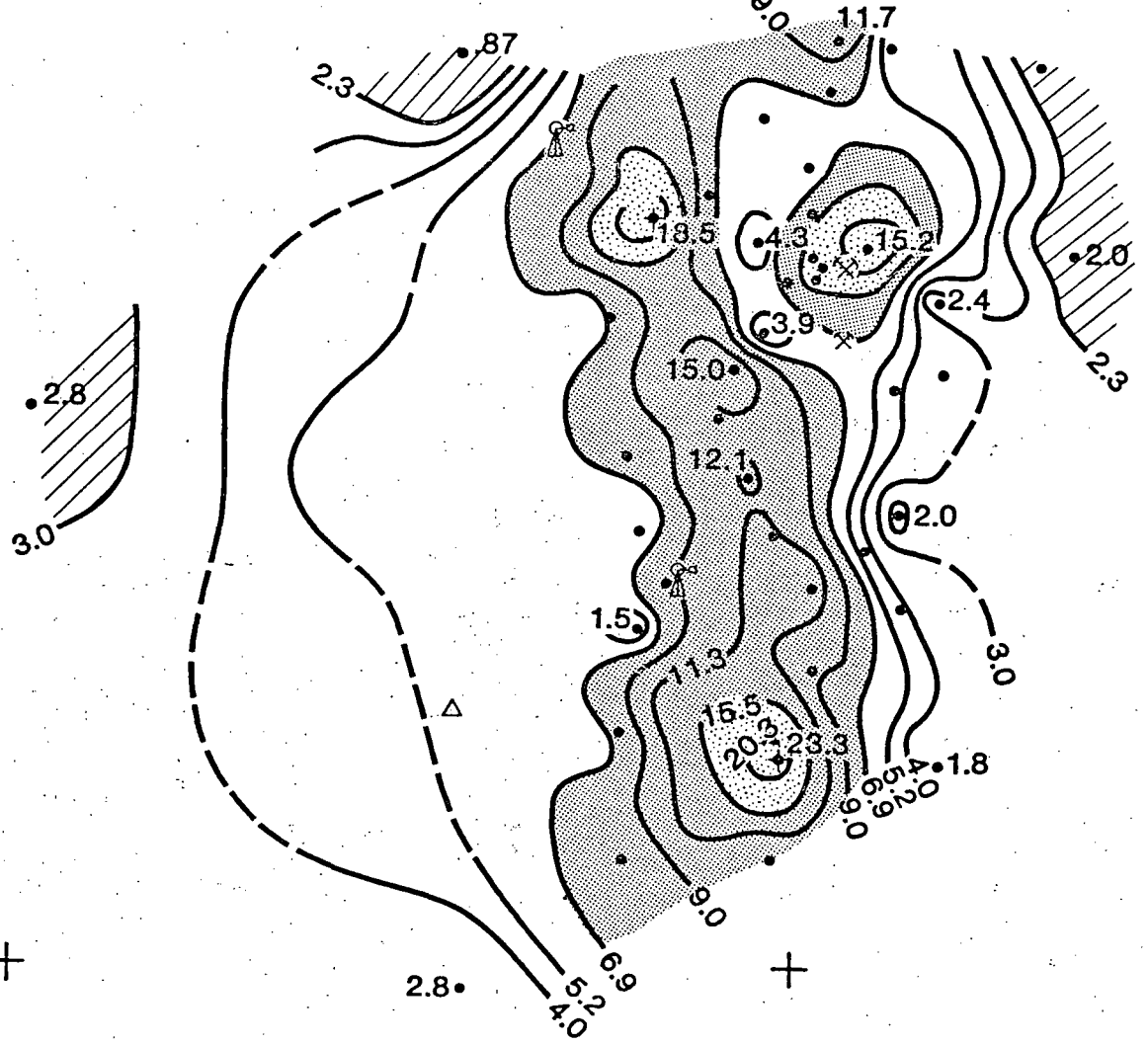
31R. MT section (T_e mode, 1D inversion) along Line C, compared with geologic section

39° 55' +

—117° 40'

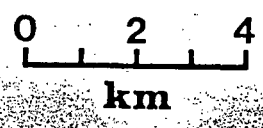
—117° 30'

39° 45' +

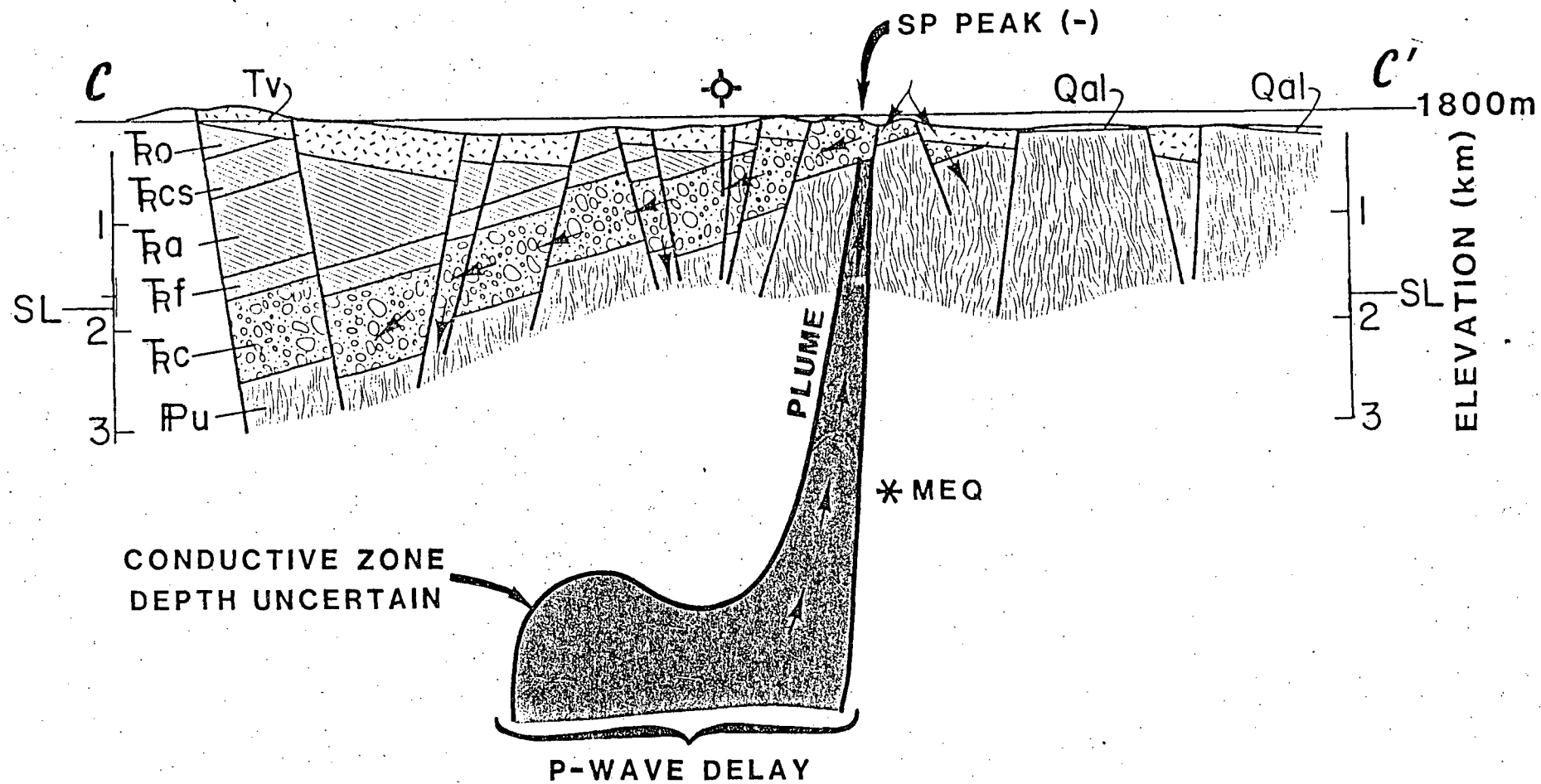


HEAT FLOW (HFU)

• WELLS



32L. Refer to Figure 8L



33R. Geologic section along Line C, showing deduced geothermal reservoir feeding conduit of ascending hot water along limb of horst block. Upon encountering the Triassic conglomerate, hot water (probably cooled by cold meteoric water from the surface) drains westward--downdip--to eventually return to the deep system.

THE McCOY, NEVADA GEOTHERMAL PROSPECT

An Interim Case History

PART III (Plates)

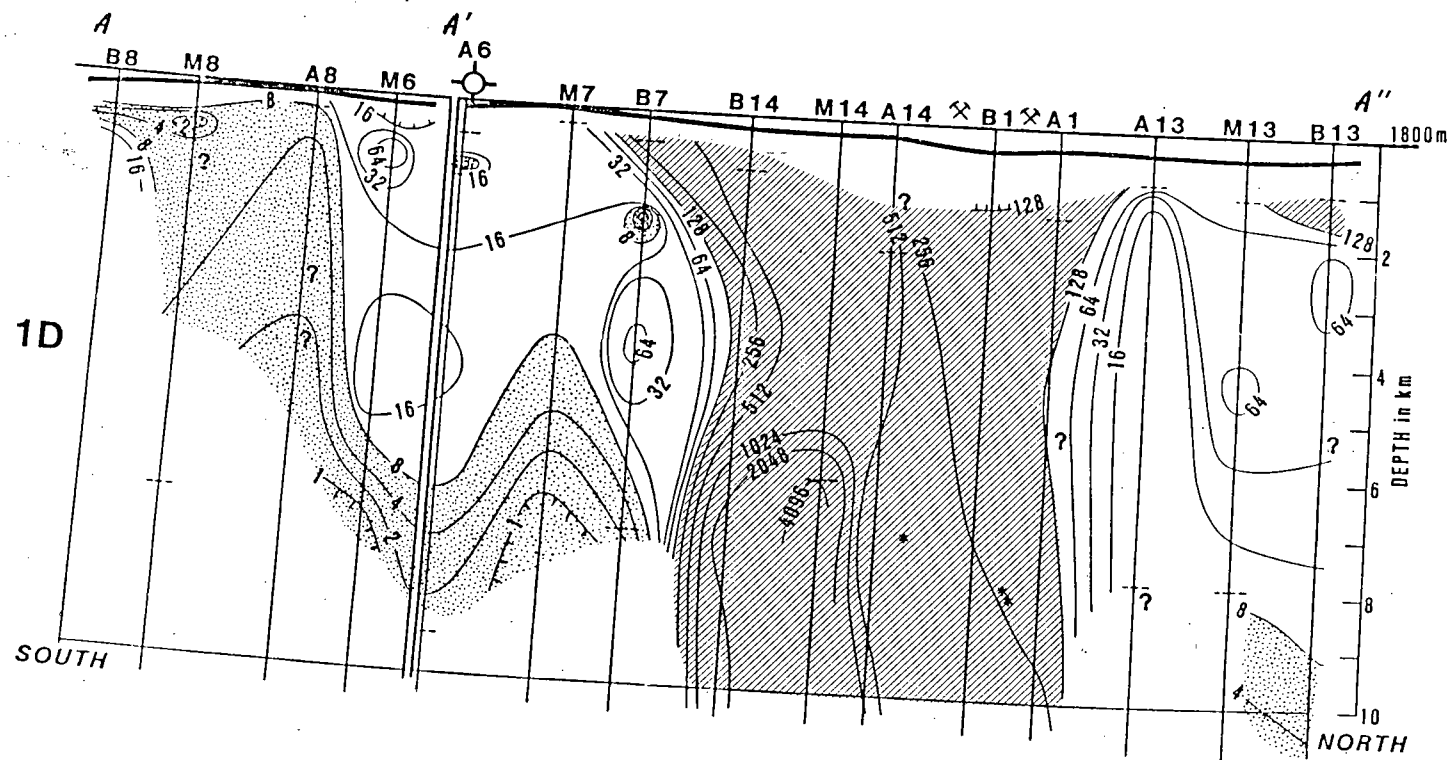
by Arthur L. Lange

*Paper delivered at the Fiftieth Annual Meeting
of the Society of Exploration Geophysicists,
Houston, Texas, 17 November 1980.*

AMAX Exploration Inc.
Geothermal Branch
7100 W. 44th Avenue
Wheat Ridge, Colorado 80033

°C
60
50
40
30

TEMPERATURE AT 100m



MAGNETOTELLURIC